SLAC-PUB-1733
April 1976

CONSTITUENT MODELS AND LARGE TRANSVERSE MOMENTUM REACTIONS*

Stanley J. Brodsky
Stanford Linear Accelerator Center
Stanford, California 94305

1. Introduction

If we assume the correctness of the quark model for the underlying structure of hadrons, then a crucial problem of particle physics is how to develop tools which can probe the hadronic interactions of the constituents at a fundamental level. Most of hadronic phenomenology gives valuable but only indirect information on quark interactions. For example:

1. The spectroscopy of hadrons yields important constraints on the large distance confinement potential--the complete ψ spectrum should turn out to be as important to quark dynamics as positronium is to QED.
2. High energy hadron-hadron interactions are consistent with the quantum number flow (i.e., duality graphs) dictated by the quark model, but the typical interactions at small t or u involve coherent multi-particle amplitudes and are difficult to analyse directly in terms of constituent interactions. Because of the Feynman dx/x spectrum the interacting particles usually only have a small fraction of the incident energy $[s_{eff} \simeq x_a x_b s \sim O(m^2)]$, and most energy is lost in beam fragmentation.

*Work supported by the Energy Research and Development Administration.

(Extracted from the Proceedings of Summer Institute on Particle Physics, SLAC Report No. 191, November 1975)

3. Deep inelastic lepton processes determine the electromagnetic and weak interactions of the constituents, and together with the elastic form factors provide important constraints on the nature of the hadronic wave function at large momentum transfer. In particular, Bjorken scaling implies that a non-zero fraction of a nucleon's momentum can be carried by a single point-like constituent.

4. Accordingly, in the case of high energy hadron-hadron collisions, particles can be produced at large transverse momentum $p_T = \sqrt{tu/s}$, by a single, hard, large angle reaction involving the point-like constituents. Note that the interacting particles must have $s_{eff} \cong x_a x_b s > 4p_T^2$. Thus if the impulse approximation is applicable--as is the case for super-renormalizable and asymptotic freedom field theories--then large p_T reactions, both exclusive and inclusive, can provide direct clues to the short distance structure of the constituents' dynamics.

In fact the emerging features of high p_T data: sets, fixed angle scaling, power behavior, etc., give strong support to the hard scattering models. Excellent discussion of these features may be found in the lectures of Bjorken[1] and Davier[2] in these proceedings. A general review of the data and an overview of various theoretical models may be found in the Physics Report by Sivers, Blankenbecler and myself.[3]

In this lecture I will make the simplifying assumptions that (1) large p_T reactions can be analyzed in terms of short distance interactions-- independent of the large distance confinement problem, and (2) that the basic quark-quark interactions within a hadron is scale-independent (modulo logarithms) as in asymptotic freedom gauge theories. A dynamical realization of these assumptions is the constituent interchange model[4] (CIM) together with the dimensional counting rules.[5,6] The CIM is a dynamical realization of the duality diagrams and thus is consistent with the usual Regge phenomenology of hadronic interactions. I will review the structure of the CIM, proofs of the counting rules, and recent phenomenological applications, including electromagnetic processes, correlations, and nuclear target effects. A new argument, "minimal neutralization", is also presented to account for the empirical absence of gluon interactions between quarks of different hadrons.

2. The Structure of Hard Scattering Models[7]

The basic assumption of the parton description of large transverse momentum reactions is that the required large momentum transfer occurs only once--in an underlying two-body reaction $a + b \to c + d$. The remainder of the process involves (Feynman-scaling) fragmentation of the in- and outgoing particles with small mean transverse momentum. This assumption can be justified if the Born interaction cross section falls with energy, as in multiperipheral models (based on super-renormalizable field theories) and the CIM. We thus have (see Fig. 1) for $p_\perp^2 \gg |\vec{k}_\perp^2|$ the simple probabilistic formula[4,8]

$$E \frac{d\sigma}{d^3p}(A + B \to C + X)$$

$$= \sum_{ab \to cd} \int_0^1 dx_a \int_0^1 dx_b \int_0^1 \frac{dx_C}{x_C^2} \, G_{a/A}(x_c)\, G_{b/B}(x_b)\, \tilde{G}_{C/c}(x_C)$$

$$\cdot \frac{d\sigma^I}{d^3p/E'} \cdot (a + b \to c + d)\Big|_{s'=x_a x_b S,\; t'=(x_a/x_C)t;\, u'=(x_b/x_C)u}$$

with $p_T^2 = tu/s$, $\epsilon = \mathcal{M}^2/s = 1 + u/s + t/s \to 1 - x_T$ at 90°. The process $a + b \to c + d$ is irreducible in that no hadronic bremsstrahlung is allowed before interaction. The variable x is the light-cone variable

$$x_a = \frac{p_a^{(+)}}{p_A^{(+)}} \equiv \frac{p_a^o + p_a^z}{p_A^o + p_A^z} \qquad (2.2)$$

(where $\vec{p}_A$ is along z), i.e., the infinite momentum fraction in a frame where $|\vec{p}_A| \to \infty$. The distribution $G_{a/A}(x_a)$ is the probability $dN_{a/A}(x_a)$ to find the (spacelike) daughter a with fraction x_a; the usual

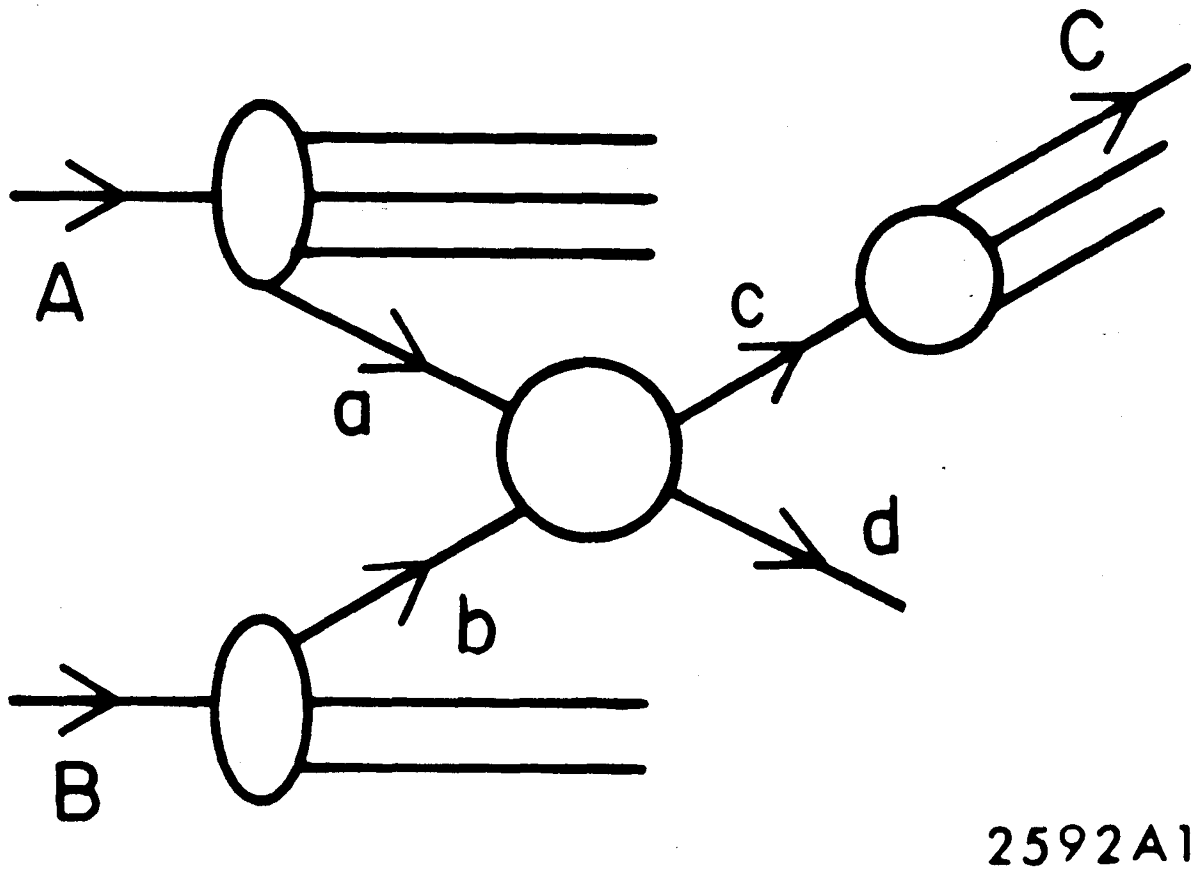

Figure 1. Structure of the hard-scattering models for the inclusive reaction $A + B \rightarrow C + X$ at large transverse momentum. The process $a + b \rightarrow c + d$ is the irreducible large angle subprocess.

quark-parton model result for $ep \to eX$ is

$$\nu W_2(x) = \sum_i Q_i^2 \, x \, G_{q_i/p}(x) \tag{2.3}$$
$$x = -t/(\mathcal{M}^2 - t).$$

The distribution $\tilde{G}_{C/c}(x_C)$ is the final state fragmentation probability $dN_{C/c}(x_C)$ to produce C from the (timelike) state c. A great number of formal properties can be derived for the G functions, using conservation laws and crossing properties:

$$\begin{aligned}
&\sum_{a\in A} \int_0^1 dx_a \; x \; G_{a/A}(x) = 1 && \text{momentum conservation} \\
&\sum_{a\in A} \int_0^1 dx_a \; Q_a \; G_{a/A}(x) = Q && \text{conserved quantum number} \\
&G_{a/B} = \int_x^1 \frac{dz}{z} \sum_{b\in B} G^I_{a/b}\left(\frac{x}{z}\right) G_{b/B}(z) && \text{convolution} \\
&G_{a/A} = \pm z \tilde{G}_{\bar{A}/\bar{a}}\left(\frac{1}{z}\right) && \text{crossing}
\end{aligned} \tag{2.4}$$

(where the $+$ sign occurs if $\bar{a} + A$ is a fermion). An extensive discussion and review is given in Ref. 3. In general there is a connection between the behavior of $G(x)$ at $x \to 0$ and the Regge behavior of total cross sections: If $\sigma_{\bar{a}A} \sim s^{\alpha-1}$ then $G_{a/A}(x) \sim cx^{-\alpha}$ $(x \to 0)$. Inserting this into (2.1), we see that Pomeron exchange, $\alpha = 1$, gives Feynman scaling for the inclusive cross section (s-independence at fixed $p_\perp$).

Since the G's are independent of scale, the scaling of the irreducible process at fixed angle,

$$\frac{d\sigma}{d^3p/E}\,(a + b \to c + d) = \frac{1}{\pi}\,\delta\left(1 + \frac{t'}{s'} + \frac{u'}{s'}\right)\frac{d\sigma}{dt'} \tag{2.5}$$

$$\to \frac{1}{(s')^{N_{abcd}}}\, f(\theta_{cm}),$$

$$s' \to \infty,\ t/s' \ \text{fixed}$$

implies

$$\frac{d\sigma}{d^3p/E}\,(A + B \to C + D) \Longrightarrow \sum_{abcd} \frac{1}{(p_T^2)^{N_{abcd}}}\, f(\theta_{cm}, \mathcal{M}^2/s) \tag{2.6}$$

at fixed θ_{cm} and $\mathcal{M}^2/s$. For example, N is equal to 2 for the scale-invariant $q + q \to q + q$ subprocess. The experimental situation (see section 6), however, shows that for the presently accessible energies no single N can accommodate all the data, e.g., for $pp \to \pi X$ at 90°, one finds $N \sim 4$ at the ISR[9,10] $(0.1 < x_T < 0.35)$ and $N \sim 6$ at FNAL[11] $(0.3 < x_T < 0.6)$. Clearly, if the quark-parton model description is relevant, a number of terms of varying N must be involved, involving various distinguishable processes which are not scale invariant. Fortunately, simple quark counting rules can be used to sort out the myriad possibilities.

3. Dimensional Counting Rules for Large p_T Reactions[4,5,7]

A unique feature of the dimensional counting rules is that the dynamical behavior of hadronic reactions--the power dependence of scaling laws and threshold dependence--can be directly related to the degree of complexity of the interacting particles.

The basic rule is as follows: First one counts the number of "active" elementary fields (quark, lepton, photon) participating in the large p_T irreducible subprocesses (see Fig. 1)

$$n_{active} = n_a + n_b + n_c + n_d \tag{3.1}$$

and the number of spectators or passive fields in A, B, and C:

$$n_{spectator} = n(\bar{a}A) + n(\bar{b}B) + n(\bar{C}c) \tag{3.2}$$

Then following the guide of Born graphs in renormalizable field theory, one finds the contribution

$$\frac{d\sigma}{d^3p/E} \to \frac{1}{(p_T^2 + m^2)^N} f(\theta_{cm}, \epsilon) \tag{3.3}$$

for $p_\perp^2 \gg m^2$, θ_{cm} and $\epsilon \equiv \mathcal{M}^2/s$ fixed. Furthermore, $f(\theta_{cm},\epsilon) \to f(\theta_{cm})\epsilon^F$ for $\epsilon \to 0$ where[5]

$$N = n_{active} - 2 \tag{3.4}$$

and[4]

$$F = 2n_{spectator} - 1 \tag{3.5}$$

The latter rule is equivalent to $G_{a/A}(x) \sim (1-x)^{2n(\bar{a}A)-1} \sim \tilde{G}_{A/a}(x)$ for $x \to 1$.

It is physically clear that N should increase as the number of fields forced to change direction increases, and that F (the degree of "forbiddenness") should increase as increasing number of spectators take away the available phase-space. The reader can readily check that the usual parton model prediction for deep inelastic processes are included as special cases here; e.g., for $ep \to eX$, $n_{active} = 4 (eq \to eq)$ and $n_{spectator} = 2$ giving $\nu W_2(x) \sim (1-x)^3$ at $x \to 1$. For scattering on antiquarks in the proton, $n_{passive} = 4$, and[12] $\nu W_2(\bar{q})\ (x) \sim (1-x)^7$. (Note that we also predict scale-breaking terms from the subprocess $e(qq) \to e(qq)$ $(n = 6)$ yielding a term $\nu W_2 \sim (1-x)/(Q^2 + m_0)^2$. Such a term may be useful in parametrizing scale-breaking near $x \sim 1$, instead of forms which use the variable $\underset{\sim}{\omega} = (2m\nu + M^2)/Q^2$, and do not retain the kinematic boundary at $x = 1$.) For the Drell-Yan process $pp \to \mu^+\mu^-X$, one has $d\sigma/d^3p/E(pp \to \mu^+X) \sim p_\perp^{-4}\epsilon^{11}f(\theta_{cm})$, and thus $d\sigma/d\mathcal{M}^2(pp \to \mu^+\mu^-X) \sim \mathcal{M}^{-4}(1 - \mathcal{M}^2/s)^{11}$. The x_L and p_T distribution of the pair are also easily predicted. A complete discussion of the counting rules for the general pair production process $A + B \to C + D + X$ is given in Ref. 13. Additional applications to e^+e^- colliding beam final states will be given in Ref. 14.

(1) There are two complications which should be kept in mind when using the spectator rule:

The derivation of the rule Eqn. (3.5) assumes that the spectators are all bound with hadrons in order that the integration over transverse momentum of the spectator converges. In the case of point-like electromagnetic couplings such as $e \to e\gamma$ the corresponding transverse momentum integration is logarithmically divergent, and the $G_{a/A}$ distributions acquire the usual logarithmic factors of the equivalent-photon/lepton (Weisacker-Williams) distributions. The spectator rule then becomes[7]

$$F = 2n_{spec}^{bound} + n_{spec}^{leptons} - 1 \tag{3.6}$$

where $n_{spec}^{leptons}$ only counts the number of unbounded spectator leptons, but not photons. With this extension, the counting rules can be applied to all the tree-graph QED processes, as well as bound state (QED or hadronic) reactions. The results agree with the equivalent photon/lepton analyses of Refs. 15 and 16. A simple example is

$$E\frac{d\sigma}{d^3p}\,(ee\to\mu^-X)\sim\frac{\alpha^4}{p_T^4}\log^2\frac{s}{m_e^2}\;\epsilon^1 \qquad (3.7)$$

where $n_{active}=4$, $n_{spec}^{leptons}=2$ for any of the contributing subprocesses: $\gamma+\gamma\to\mu^+\mu^-$, $\gamma e\to\gamma e$, $e\mu\to e\mu$. If the incident particles are both positronium atoms, the ϵ power is increased by 4 to ϵ^5 since $n_{spectators}^{bound}=2$. Note that extra photon spectators do not change the ϵ dependence because of their infrared dk/k coupling. The same result clearly also holds for the soft vector gluons radiated by quark lines.

(2) The rule (3.6) is formally inconsistent with the sign of the crossing relation in (2.4) if the spectator system has the quantum numbers of a fermion. Indeed in Bethe-Salpeter calculations of the bound state of two fermions, one finds[17] $G_{q/\pi}\sim\nu W_2^\pi\sim(1-x)^2$ instead of $(1-x)$, with an extra cancellation at $x\sim1$ forced by helicity and spin conservation.[18] However, the non-leading term $\nu W_2^\pi\sim(1-x)^0\langle k_\perp^2\rangle/Q^2$ though non-leading at large Q^2, has the effect of a $(1-x)^1$ term at $\mathcal{M}^2/Q^2\to0$. For convenience, then, we shall retain the rule (3.6) in phenomenological comparisons, although formally the spin complications and rearrangement of terms at $\epsilon\to0$ should be kept in mind. In any event, the exclusive-inclusive connection (see Section 6) is satisfied. A more detailed discussion will be given elsewhere.[14]

4. Dimensional Counting and Exclusive Processes

In the case of exclusive processes, the number of spectators is zero and dimensional counting implies[5,6]

$$\frac{d\sigma}{dt}(A + B \to C + D) \to \frac{1}{s^{n_A+n_B+n_C+n_D-2}} f_{A+B\to C+D}(\theta_{cm}) \qquad (4.1)$$

for the general two-body reaction. Applied to electron scattering, this gives

$$F_{H}(t) \sim t^{1-n_H}, \qquad t \to \pm\infty \qquad (4.2)$$

for the spin-averaged form factor of a bound state of n_H fields. Alternatively, using quark counting for any exclusive reaction $A + B \to C + D + \cdots Z$, we can write[5]

$$\Delta\sigma \to s^{-1-N_M-2N_B}, \qquad s \to \infty \qquad (4.3)$$

for the cross section integrated over any fixed angle region with each $p_i \cdot p_j / s$ $(i \neq j = A, B, \ldots, Z)$ finite. (This last relation is particularly interesting for e^+e^- annihilation, e.g., $e^+e^- \to N(\pi)$ above the resonance contributions.) N_M and N_B are the number of mesons and baryons respectively in the initial and final states.

The tests of dimensional counting for two body reactions are reviewed extensively in Davier's lectures in this proceedings[2] and in Refs. 3,19. Thus far there is no clear contradiction with the predictions, although higher energy tests are definitely needed. It may be possible to increase the range of the tests in experiments covering large CM solid angle or using nuclear targets (see Section 16).

A very recent test of fixed angle behavior is the measurement of $"\gamma"(q^2) + p \to \pi + p$ by Hansen et al. at Cornell.[20] They find $d\sigma/dt \propto s^{-7.5 \pm 0.4}$ at $(E_\gamma^{Lab} < 12$ Gev), $\theta_{cm} = 90^\circ$, for $|q^2|$ up to ~2 Gev^2, in agreement with the fixed angle photoproduction measurement $d\sigma/dt(\gamma p \to \pi p) \propto s^{-7.3 \pm 0.4}$ by R. Anderson et al. at SLAC.[21] Note that the dimensional counting prediction is s^{-7} for asymptotic s, θ_{cm} fixed, with $|q^2| << |t|$. When $q^2 \sim O(t)$, one may compare directly with Eq. (4.3) $\Delta\sigma(ep \to e\pi p) \sim s^{-5}$.

An important question is what momentum transfer is sufficient to make a fair comparison with the scaling laws without including mass corrections, etc. In the case of the elastic form factor of the proton (see Fig. 2), one sees that for $5 > -t > 25$ Gev^2, $t^2 G_M$ is consistent with a constant within 5%. The scaling $d\sigma/dt(pp \to pp) \sim s^{-10} f(\theta_{cm})$ is reasonably good for $|t| > 4$ Gev^2. In the case of non-exotic channels, e.g., $\pi^+ p \to \pi^+ p$, $p\bar{p} \to p\bar{p}$ the scaling onset is expected to be at larger t, although extrapolation of the $p_{Lab} = 10$ Gev/c $\pi^+ p \to \pi^+ p$ large angle data to 5 Gev/c, using the s^{-8} law does a good job of averaging out the resonance structure at the lower energies.[22] This illustrates a type of duality, where the fixed angle scaling law fits --on the average--the s-channel resonant contributions. The form of the fixed angle scaling function $f(\theta_{cm})$ is well-described by the CIM model (see Section 15), but not by gluon exchange. The crossing behavior relating $pp \to pp$ to $p\bar{p} \to p\bar{p}$, $K^- p \to K^- p$ to $K^+ p \to K^+ p$, etc. predicted by the power law CIM forms are also reasonably consistent with experiment.[23] It should be noted, however, that phenomenological forms (based on geometrical arguments and a fixed distance scale) of the type e^{-ap_T}, where a varies with θ_{cm} can also be used to parametrize the present range of two body scattering data,[24,25] although such forms have not been successfully extended to fit inclusive data.[26]

An important feature of the large angle data which is not accounted for by the scaling laws are the presence (even at large t) of oscillations and fixed-t dips, as emphasized by Hendry[24] and Schremp and Shremp.[25] This structure is particularly striking in the plot of $s^{10}\, d\sigma/dt\ (pp \to pp)$ shown in Fig. 3. Such structure demands that a fixed distance scale influences large angle hadron scattering, and of course, is natural in geometrical models. In the context of the parton model one can think of at least two interesting possible explanations: (1) The fixed t structure is induced by the absorption or peripheral interactions of the soft parton structure of the hadrons. (2) The confinement of the quarks within a fixed distance (as in bag models) induces an oscillatory structure in the quark propagator, which in turn modifies the parton model amplitudes. Nuclear targets and phase measurements can be used to discriminate these possibilities. The latter possibility will be discussed in more detail elsewhere.

5. The Deuteron Form Factor

In principle the dimensional counting prediction should hold even for nuclear states in the asymptotic short distance region where constituent interactions are dominant. The prediction for asymptotic behavior of spin-averaged deuteron form factor is $(n = 6)$[5]

$$F_D(t) \sim t^{-5} , \qquad t \to -\infty \tag{5.1}$$

where

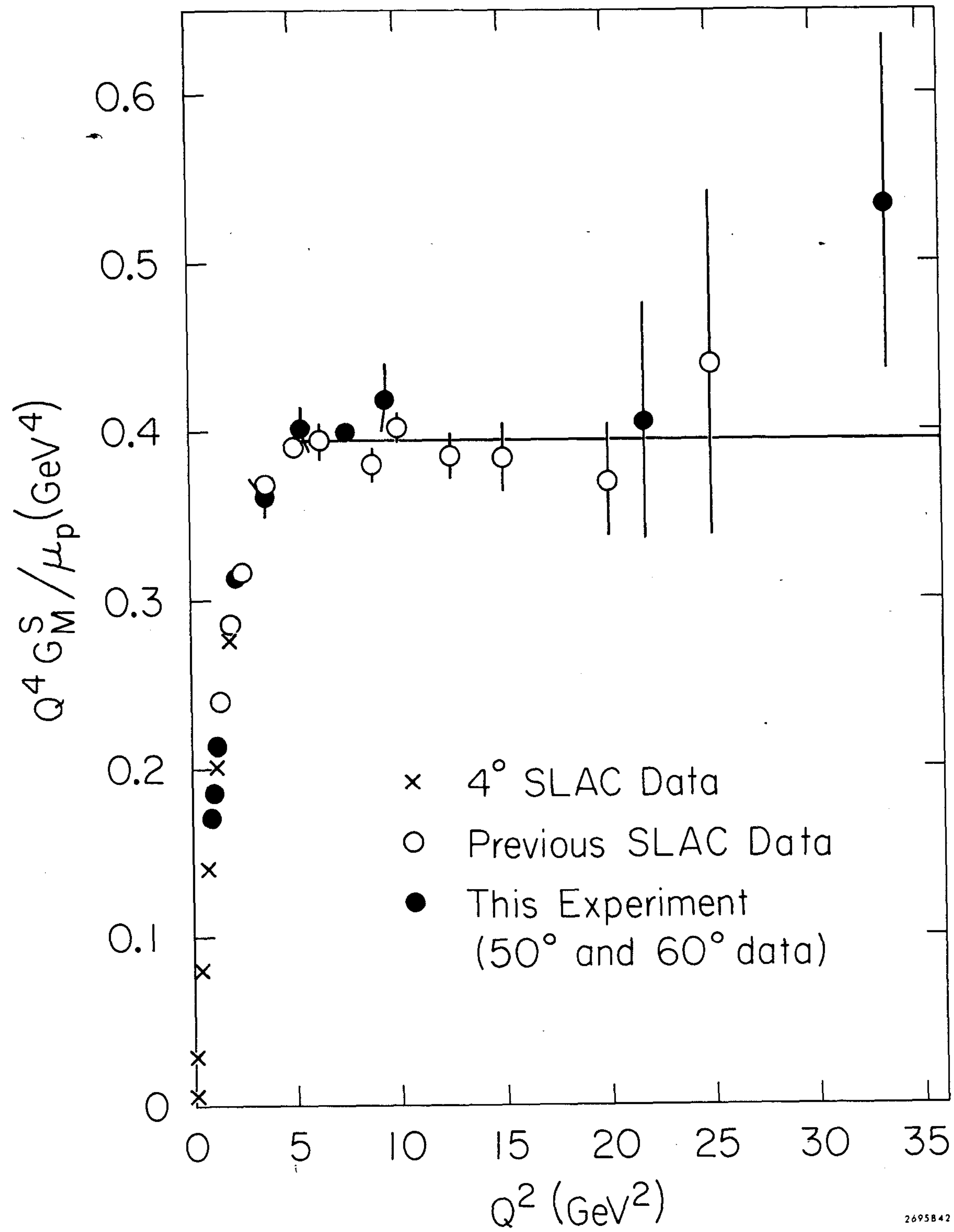

Figure 2. A plot of $Q^4 Gm$ /exp versus Q^2. The dashed line is the usual dipole fit. The solid line is fit given by W. Atwood with $Q^4 Gm \rightarrow$ const. From W. Atwood, SLAC-185 (1975).

$$\frac{d\sigma}{dt} = \frac{4\pi\alpha^2}{t^2} [F_D^2(t) + 0(\frac{t}{s}) \ldots] \tag{5.2}$$

Furthermore since each nucleon must change directions from approximately $p/2$ to $(p + q)/2$ we predict[27]

$$F_D(t) \cong F_N^2(\frac{t}{4}) \frac{1}{1 - t/m_0^2} \tag{5.3}$$

where m_0^2 is a scale set by an off-shell quark propagator. A typical "partition" diagram (see Sec. 12) is shown in Fig. 4. Note that this diagram allows for quark rearrangement between the nucleons in the short distance regime,and the gluon exchange only needs to occur within the confines of the nucleon wavefunction.

The deuteron form factor has been measured at $-t$ up to 6 Gev^2 by Arnold et al. using a double spectator system at SLAC. A fit to the asymptotic behavior t^{-N} gives $N = 5 \pm 0.6$.[29] Figure 5 shows that the ratio $F_D(t)/[F_N^2(t)\ (1 - t/m_0^2)^{-1}]$ with $m_0 = 300$ Mev indeed flattens to a constant value as predicted--but at a surprisingly low value. In contrast, calculations of meson exchange contributions falloff too slowly compared to the data; the dimensional counting rules and the partition diagram of Fig. 4 provide a consistent calculation of the effective exchange current contributions. The counting rules also predict $G_{p/d}(y) \sim (1 - y)^5$ $(n_{spect} = 3)$ for the fall-off the fermi momentum for $y \sim 1$, the region where the proton carries nearly all of the deuteron momentum. This can be tested in $eD \rightarrow eX$ and in $Dp \rightarrow pX$ in the deuteron fragmentation region.

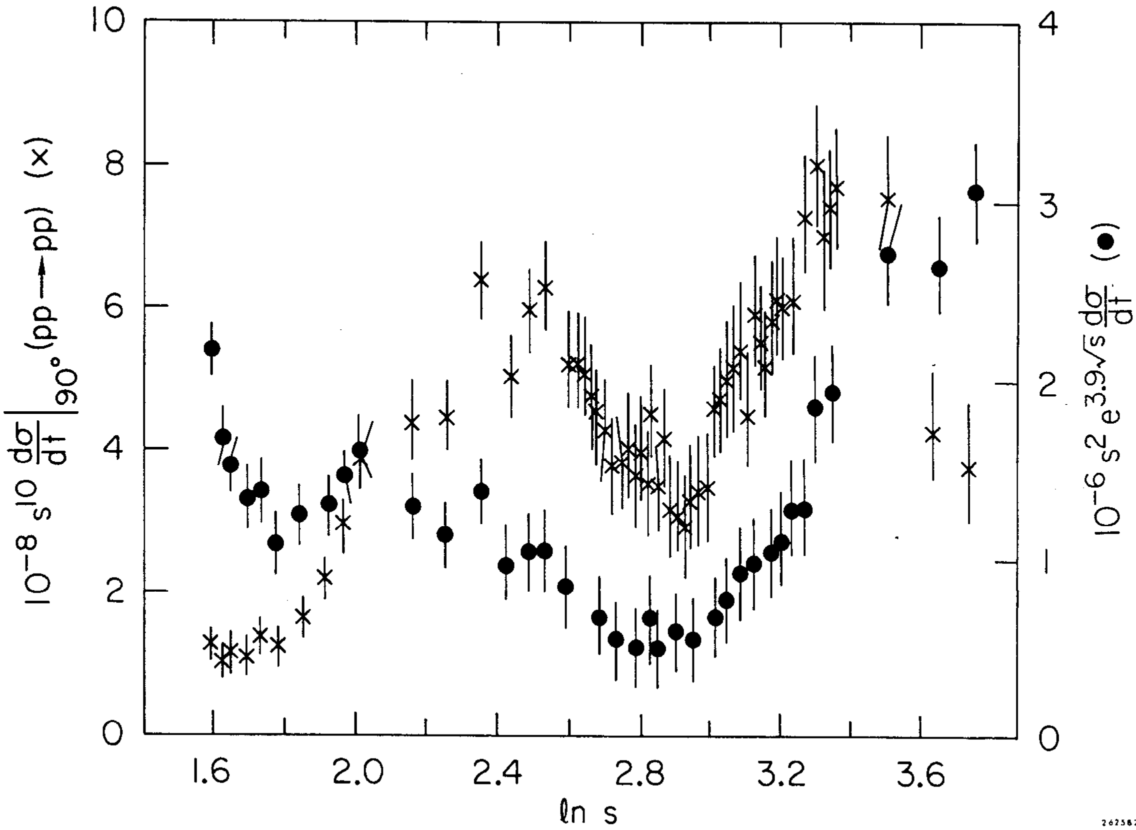

Figure 3. Plot of S^{10} $d\sigma/dt$ $(pp \to pp)$ (x), and $e^{3.9\sqrt{s}}$ $d\sigma/dt$ (.), showing oscillations at fixed t. (From ref. 3.)

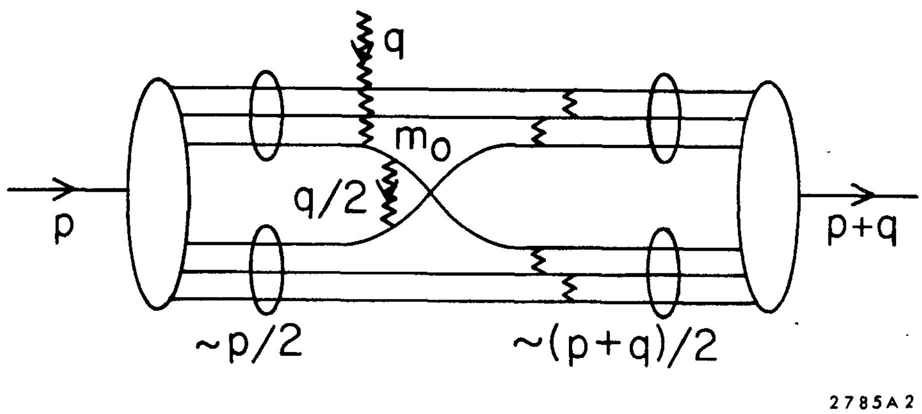

Figure 4. Partition contribution to the deuteron form factor which is consistent with color symmetry. The nucleons change momentum from $p/2$ to $(p + q)/2$.

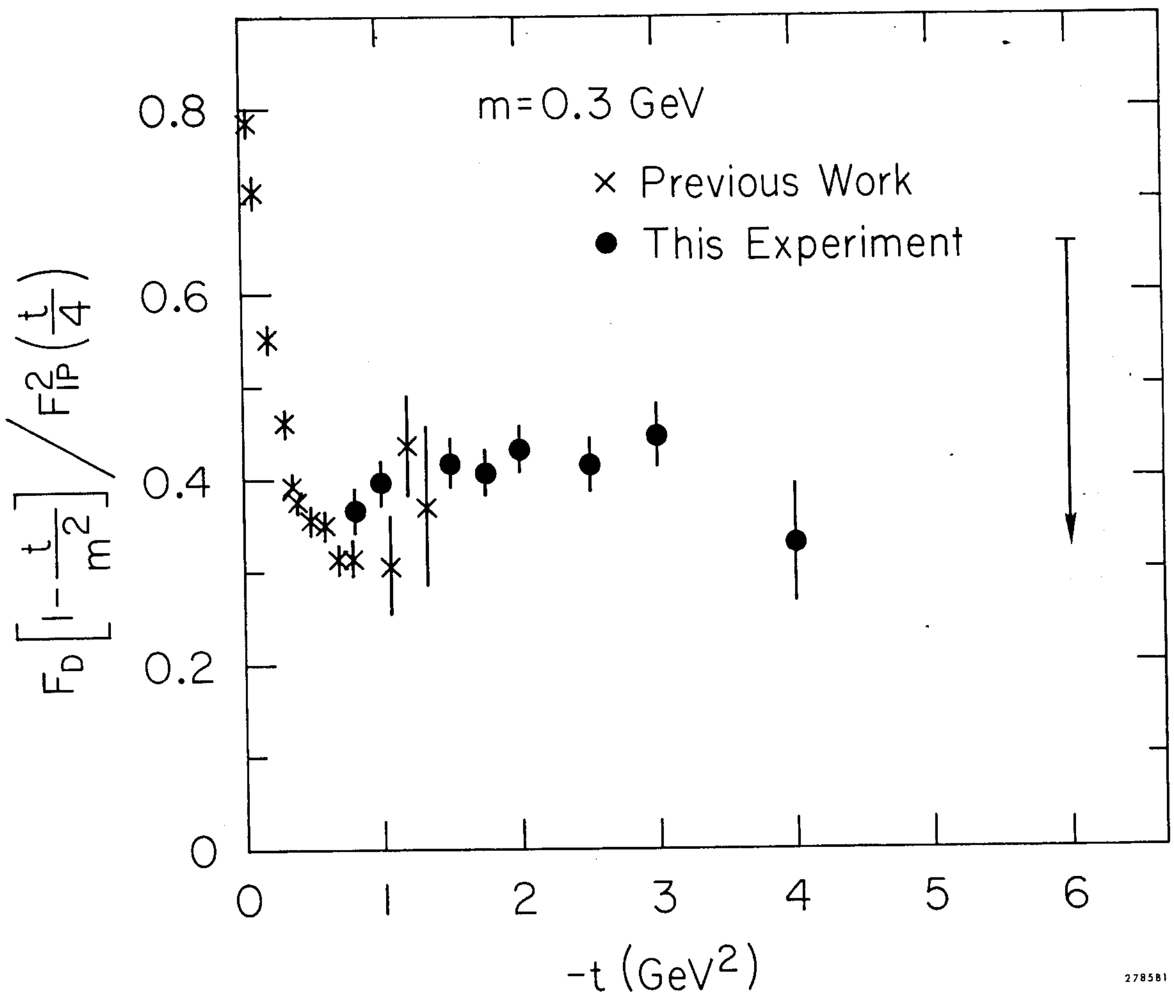

Figure 5. Ratio of Arnold et al. data to the dimensional counting prediction.

6. Applications to Inclusive Reactions[31]

If we use the dimensional counting rules, then the quark model predicts a sum of terms

$$E\frac{d\sigma}{d^3p}(A+B\to C+X)=\sum_{ab\to cd}\frac{C_{abcd}}{(p_T^2+m^2)^{N_{abcd}}}f_{abcd}(\theta_{cm},\epsilon) \qquad (6.1)$$

where $N = n_{active} - 2$ can be 2, 4, 6, etc. Possible reasons why a p_T^{-4} scale-invariant term $(N = 2)$ from $q+q\to q+q$ is not observed in the present data range of the FNAL and ISR are discussed in Section 14. In the CIM, the important subprocesses of a hadronic reaction are postulated to invariably involve at least one hadronic wavefunction--as would be natural in a bag model. The subprocesses with the minimum fall-off have six active quarks corresponding to $q+M\to q+M$ and $qq\to B+\bar{q}$ and their crossing invariants. Thus for any hadronic process, the CIM predicts $p_T^8 E\, d\sigma/d^3p \to f(\theta_{cm},\epsilon)$ at large p_T. Indeed, an excellent fit to the CCR-ISR data[9] for $pp\to\pi^0X$ can be obtained from Eq. (6.1) with $G_{\pi/p}\sim(1-x)^5$, $G_{q/p}\sim(1-x)^3$ giving $E\,d\sigma/d^3p\sim(p_T^2+M^2)^{-4}\,\epsilon^9$ for the subprocess $q\pi\to q\pi$ with $n_{spectators}=5$. The same predictions hold for $pp\to(\pi^\pm,K^+)+X$, but for K^- production, an extra two spectators are required. Thus we predict at large p_T, and small $\epsilon\equiv\mathcal{M}^2/s$

$$\frac{d\sigma(pp\to K^-X)}{d\sigma(pp\to K^+X)}=\epsilon^4 f(\theta_{cm}) \qquad (6.2)$$

These results can be directly compared with the recent British-Scandinavian results[10] at the ISR (see Table I). Some caution is needed here since ϵ $(=1-x_T$ at $90^0)$ is ≥ 0.75, and thus is too large to adequately test the F power, which is defined for $\epsilon\to 0$. Nevertheless,

TABLE I[10]

Fits to the Function $A(1 - p_T/p_{beam})^F/(p_T^2 + m^2)^N$

Particle	A	m	F	N	χ^2 NDF
π^+	6.9 ± 0.7	0.86 ± 0.02	11.0 ± 0.7	3.85 ± 0.06	532/198
π^-	7.4 ± 0.7	0.89 ± 0.02	11.9 ± 0.7	3.89 ± 0.07	604/199
K^+	9.9 ± 2.3	1.30 ± 0.04	9.0 ± 1.0	4.36 ± 0.15	245/107
K^-	10.4 ± 4.2	1.33 ± 0.08	12.2 ± 1.1	4.38 ± 0.18	198/107
p	52 ± 14	1.35 ± 0.05	7.3 ± 0.9	5.19 ± 0.17	233/110
$\bar{p}$	9.0 ± 2.6	1.08 ± 0.05	14.0 ± 1.4	4.55 ± 0.15	287/110
			Fits with N fixed		
π^+	8.1 ± 0.5	0.90 ± 0.01	9.7 ± 0.4	4.0	537/199
π^-	8.2 ± 0.6	0.92 ± 0.01	11.0 ± 0.4	4.0	606/200
K^+	4.8 ± 0.6	1.17 ± 0.03	10.4 ± 0.7	4.0	251/108
K^-	4.6 ± 0.8	1.18 ± 0.04	13.6 ± 0.9	4.0	202/108
p	5.3 ± 0.7	0.94 ± 0.03	12.1 ± 0.7	4.0	308/111
p	380 ± 65	1.59 ± 0.03	5.7 ± 0.8	6.0	251/111
$\bar{p}$	3.4 ± 0.6	0.88 ± 0.04	16.5 ± 1.2	4.0	296/111
$\bar{p}$	296 ± 75	1.55 ± 0.04	11.5 ± 1.4	6.0	318/111

the results are certainly consistent with the CIM predictions. Note that the experimental value of the ratio (6.2) is $\epsilon^{3 \pm 1}$. The parameter m ~~is~~ ~ O(1 Gev) which is in a comfortable range.

We note that the British-Scandinavian results do not indicate presence of the contribution $(p_\perp^2 + m^2)^{-4} \epsilon^7$ expected for $pp \to pX$ from the $qq \to p\bar{q}$ subprocess. This process, like $qq \to qq$, invokes double quark charge neutralization, and may be dynamically suppressed, as we argue in Section 14. The subprocess $qM \to q'M$ followed by the fragmentation $q' \to p + (q\bar{q})$ predicts $p_\perp^{-8} \epsilon^{13}$, which is consistent with the B-S data ($F = 12.1 \pm 0.7$), if the power N is constrained to $N = 4$. However the preferred power of the fit is $N = 5.19 \pm 0.17$, which we shall argue is due to the additional presence of an $N = 6$ term. The subprocesses $q + (qq) \to M + B$ and $B + q \to p + q$ give $(p_\perp^2 + m^2)^{-6} \epsilon^5$, ϵ^7, respectively. The value of the B-S fit with $N = 6$ in fact gives $F = 5.7 \pm 0.8$. A list of the predictions for the various CIM subprocesses is given in Table II. Note that the process $p + q \to p + q$ with $n_{passive} = 2$, $F = 3$, where the incident proton interacts directly, has its main contributions in the far forward/backward direction $x_L \sim \pm 1$ since the full beam energy is involved. Some bremsstrahlung from both A and B is needed to yield a central region contribution. In this case this increases $n_{spectator}$ to 4, $F = 7$. Thus the most important subprocesses in the CIM scheme for the ISR data range seem to be (a) $q + M \to q + M$ and (b) $q + (qq) \to M + B$. Note that for $\bar{B}$ production these give $(p_\perp^2 + m^2)^{-4} \epsilon^{15}$ and $(p_\perp^2 + m^2)^{-6} \epsilon^{11}$, respectively, which again are consistent with the B-S fits. Smaller contributions would also be expected to occur from the other CIM subprocesses listed in Table II.

TABLE II[30]

CIM Subprocesses

	Subprocess	$\pi^{\pm,0}K^{+},\rho^{\pm,0}$	F_{min} for $(pp \rightarrow)$ K^{-}	p	$\bar{p}$
N = 4	$q + M \rightarrow q + M$	9	13	13	15
	$q + \bar{q} \rightarrow M + \bar{M}$	11	11	17	17
	$q + q \rightarrow B + \bar{q}$	9	9	7	11
N = 6	$q + (qq) \rightarrow M + B$	5	9	5	11
	$q + B \rightarrow q + B$	5	9	3	11
	$M + M \rightarrow M + M$	11	11	17	17
	$q + \bar{q} \rightarrow B + \bar{B}$	17	17	11	11

The fact that more than one subprocess contributes in the CIM with different dependence on p_T and ϵ provides a simple explanation of why the effective power of N can change as one turns from the ISR range to the FNAL data range of the Chicago Princeton Group.[11] In the case of $pp \to p\pi$ the two subprocesses $q\pi \to q$ and $q + (qq) \to \pi + B$ gives a form[4]

$$\frac{d\sigma}{d^3p/E}\,(pp \to \pi X) = \frac{A}{(p_T^2 + m_a^2)^4}\,\epsilon^9 + \frac{B}{(p_T^2 + m_b^2)^2}\,\epsilon^5. \qquad (6.3)$$

(Again we emphasize that this form is simplified since the actual distributions in ϵ only approach ϵ^F for $\epsilon \to 0$. The errors this introduces are discussed in Ref. 30.) In the ISR regime where $\epsilon > 0.65$ only the first term contributes. For the FNAL data, which spans $0.4 < \epsilon < 0.7$, the second term becomes important at small ϵ despite the extra power of $p_\perp^{-4}$, and in fact dominates for fixed $\mathcal{M}^2$, $p_T \to \infty$. Good fits to the CP and BS data for $p_T > 2$ Gev/c using the form (6.3) can be obtained. At smaller p_T, the effective Regge behavior $\alpha(t)$ is predicted to rise from the CIM negative integer values and more complicated forms are required.

One of the most sensitive parametrizations of the data, providing a strong discriminant of various models, is the use of the effective powers[31,30]

$$N_{eff} = -p_T^2 \frac{\partial}{\partial p_T^2}\left[\log E \frac{d\sigma}{d^3p}\right]_{\epsilon,\,\theta_{cm}\ \text{fixed}} \qquad (6.4)$$

$$F_{eff} = \epsilon \frac{\partial}{\partial \epsilon}\left[\log E \frac{d\sigma}{d^3p}\right]_{p_T,\,\theta_{cm}\ \text{fixed}} \qquad (6.5)$$

which can be obtained as finite differences from the large p_T data at several different energies. (The form $[p_T^2 + m_0^2]^{-N} \epsilon^F$ gives $F_{eff} = F$ and N_{eff} approaching N from below for $p_\perp^2 \gg m_0^2$.) The kinematic dependence of N_{eff} and F_{eff} map the extremely fast changing cross sections into a form which is easily compared with theory. We note the following provisio concerning the CP data: (1) The proton data is obtained from the $A \to 1$ extrapolation of heavy nucleus data. (2) The measurements were made at $\theta_{cm} = 77^o, 90^o, 96^o$ for the beam momenta $p_{Lab} = 200, 300, 400$ Gev/c, rather than fixed angle. In addition, in any data, possible systematic errors, normalization changes between energies can lead to distortion in the values of N_{eff} and F_{eff}.

The results for the CP(FNAL),[11] BS(ISR),[10] and CCR(ISR)[9] data are shown in Figures 6 and 7. The values of N_{eff} and F_{eff} for the BS data agree with the more recent fits provided by the experimentalists in Table I. The large range in F_{eff} (obtained using different energy pairs) shows that these values are less certain than those for N_{eff}. The plateauing of N_{eff} for $\pi^{\pm}$ at $N = 4$ at the ISR and $N = 6$, with the corresponding drop in F_{eff} shows how the balance toward terms with more active and fewer spectators occurs as one approaches the exclusive limit of the Peyrou plot at $\epsilon \to 0$. We should mention here that the observed kinematical dependence of N_{eff} and F_{eff} and the differences among particle types is very difficult to explain in thermodynamic and statistical models. Although the linear rise in N_{eff} as $\epsilon \to 0$ as predicted by the eikonal model of Fried et al.[32] is in rough agreement with the trend of the data (although not the plateauing), the same model predicts F_{eff} to be independent of s at fixed p_T in contradiction to the ISR/FNAL comparison. Further details may be found in Ref. 30.

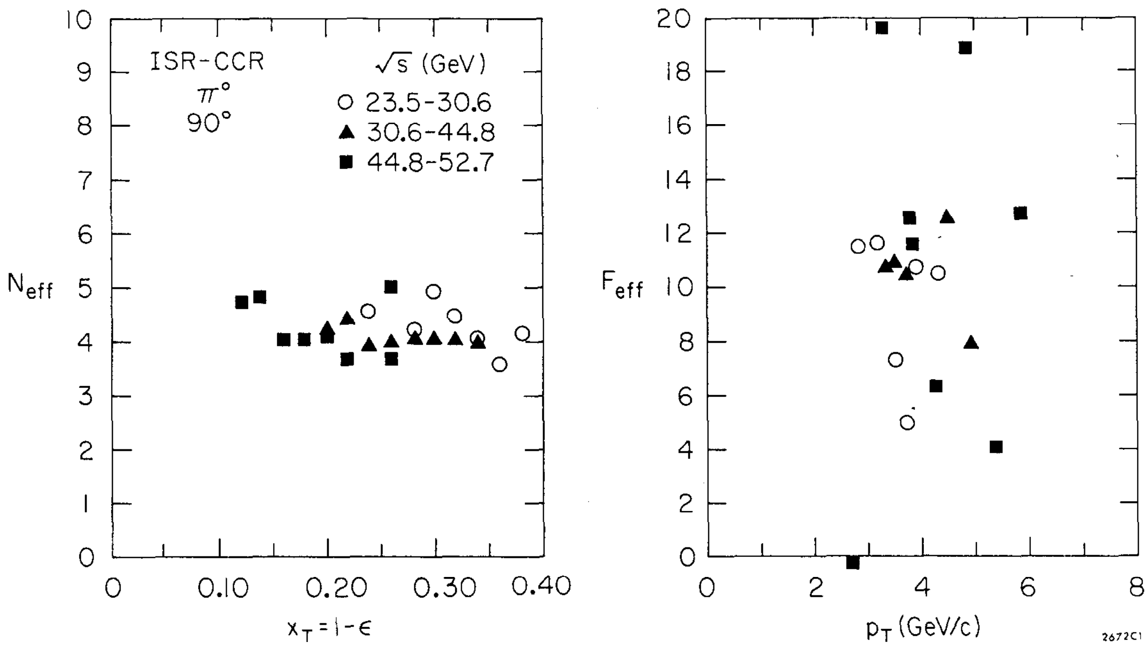

Figure 6. The parameters F_{eff} and N_{eff} obtained from the $pp \to \pi^0 X$ ISR data of CCR collaboration. Three energy pairs are used as indicated, with $p_T > 2.5$ GeV. The statistical errors are of the same size as the discrepancies from the different energy pairs. The prediction of the CIM is $N_{eff} = 4$ for this kinematic range.

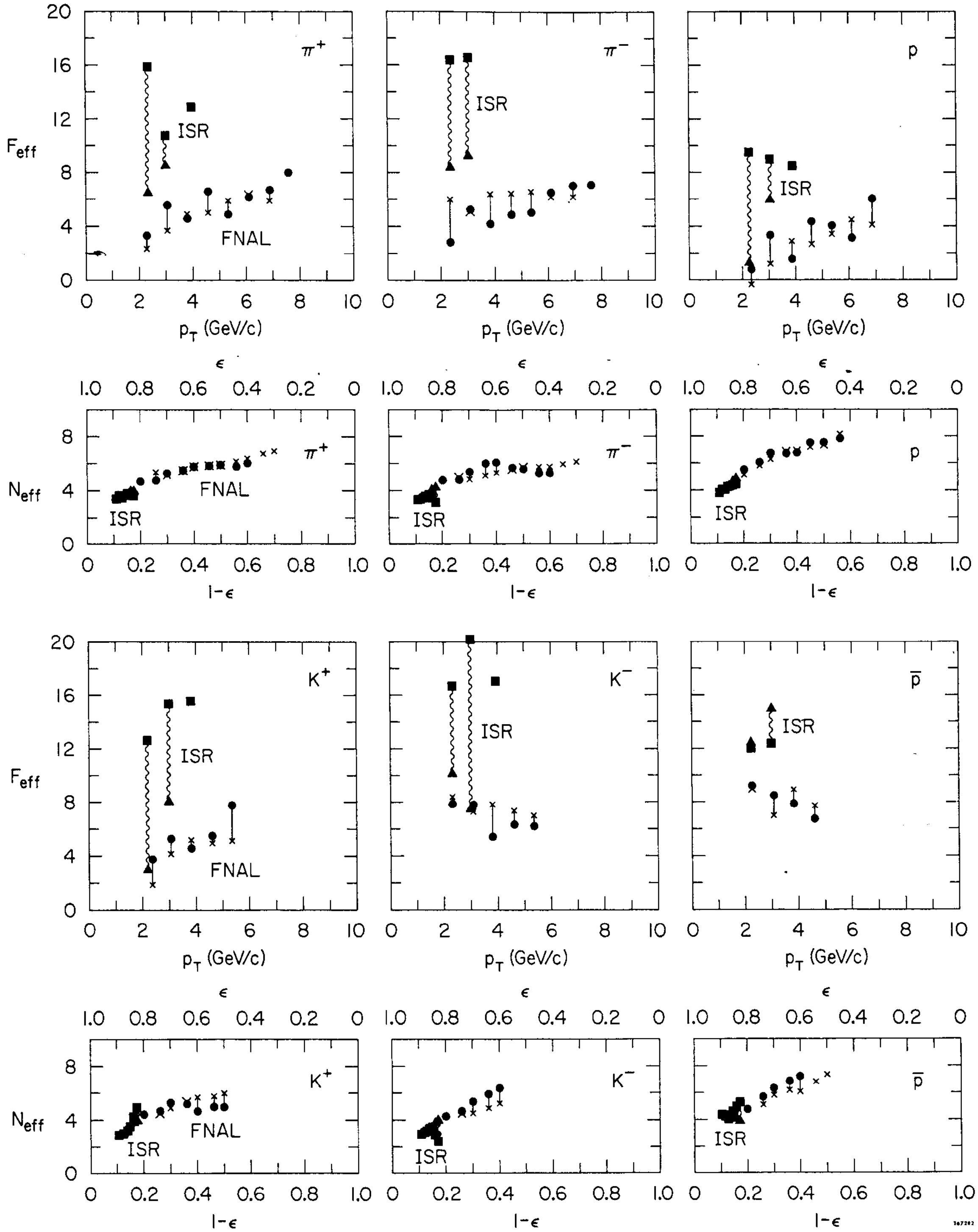

Figure 7. The parameters F_{eff} and N_{eff} for charged hadron production at the CERN-ISR BS Collaboration, pp collisions and the FNAL CP Collaboration, p_L = 200, 300, 400 GeV proton-Tungsten collisions. The energy pairs for the ISR (connected by wavy lines) are ($\sqrt{s}$ = 30.6 -44.8 GeV), and ($\sqrt{s}$ = 44.8 - 52.7 GeV). The energy pairs for the FNAL (connected by straight lines) are ($\sqrt{s}$ = 19.4 - 23.8 GeV) and ($\sqrt{s}$ = 23.8 - 27.4 GeV). A p_T dependent nuclear correction is assumed for the FNAL data. Only $p_T > 2$ GeV/c

Although the CIM subprocesses with $n_{active} = 6, 8$ can reproduce the effective powers of the meson production data, the N_{eff} curves indicate the presence of p_T^{-16} ($n_{active} = 10$) terms at the lower values of ϵ in the CP proton data. Again this shows the increasing importance of terms with more active fields and fewer spectators as one approaches the exclusive boundary, but with the total number remaining constant. The smooth connection to the exclusive limit ($\mathcal{M}^2$ fixed) requires[5,33]

$$N + F + 1 = N_{excl} = n_{excl} - 2 \tag{6.6}$$

where n_{excl} is the number of fields in the corresponding exclusive channel $A + B \to C + D(\mathcal{M}^2)$. This is the implementation of the correspondence rule of Bjorken and Kogut[34] (generalizing Bloom-Gilman[35] duality and the Drell-Yan[36] rule for electroproduction) and is obtained automatically from the counting rules (3.4, 2.5). An important prediction of the CIM for pp collisions is the ordering

$$N_{excl}(\bar{p}) > N_{excl}(\bar{K}) > N_{excl}(K^+,\pi^\pm) \geq N_{excl}(p) \tag{6.7}$$

In fact, not only the ordering, but also the values of N_{excl} from the NAL data are consistent with the quark-counting predictions! (See Table III.)

TABLE III

Comparison of $N_{eff} + F_{eff} + 1$ and N_{excl}

	ISR(BS)[10]	FNAL(CP)†	N_{excl}
p	12.5 ± 1.0	13	12(10)*
π^+	15.9 ± 0.8	12.5	12
π^-	15.8 ± 0.8	12.5	12
K^+	13.4 ± 1.1	12.5	12
K^-	16.6 ± 1.3	14	14
$\bar{p}$	18.6 ± 1.6	16	16

$^{*}N_{excl} = 10$ for $pp \to pX$ corresponds to $(pq \to pq)$ and should only dominate forward/backward angles.

†FNAL values[11] (from Fig. 7 at $p_{\perp} \sim 5$ Gev, $\epsilon \sim 0.5$ (see Ref. 30)). are uncertain by at least ± 1.

7. Predictions for Meson and Photon Beams

Some of the most crucial tests of the CIM arise in large p_T reactions with meson beams. Since the form of the hard scattering model (3.3) explicitly satisfies crossing, we can relate $A + B \to C + X$ to $\bar{C} + B \to \bar{A} + X$ by simple $s \longleftrightarrow u$ substitution. Thus $\pi^- p \to \bar{p}X$ can be completely predicted (including normalization) from the CIM parametrization for the $pp \to \pi^+ X$ data, etc.; we expect $d\sigma(\pi^- p \to \bar{p}X)/d\sigma(pp \to \bar{p}X) \sim \epsilon^{-4}$ at fixed p_T. (This also can be applied to $\bar{p}$, K^+, K^- beams.) In general a meson (or photon) beam is predicted to be more efficient than a proton beam in initiating high p_T reactions since the quark carries a larger fraction of the momentum in the meson. In general we predict

$$\frac{d\sigma(pp \to HX)}{d\sigma(\pi p \to HX)} \sim \epsilon^2 \qquad \text{at fixed } p_T, \theta_{cm} \tag{7.1}$$

for subprocesses $q + M \to q + M$, $q + (qq) \to M + B$, etc., since there is one less spectator. (We ignore $\pi + q \to \pi + q$ with no spectators from the pion, for $x_L \not\to 1$.) In particular, we expect for almost any parton model of new particle production

$$\frac{d\sigma(pp \to \psi X)}{d\sigma(\pi p \to \psi X)} \sim \epsilon^2 \tag{7.2}$$

Note that this implies the fall-off $(1 - x_L)^2$ for the ratio in the beam fragmentation region, which is consistent with what has been reported by the Northeastern experiment at FNAL.[37]

The application of the counting rules are particularly interesting for photon processes since the electromagnetic coupling gives

$$G_{q/\gamma}(x) = G_{\bar{q}/\gamma}(x) \sim \frac{\alpha}{\pi} (1 - x)^0 \log \frac{s}{m_q^2} \tag{7.3}$$

Thus we typically expect:

$$d\sigma(\gamma p \to HX):d\sigma(Mp \to HX):d\sigma(pp \to HX)$$

$$= \epsilon^0:\epsilon^1:\epsilon^2 \tag{7.4}$$

In addition there will be background terms where the photon acts as a meson beam. It is also interesting to test these predictions in cases where H is a wide angle lepton pair.

The application of the CIM to $\gamma p \to \gamma X$ and $\gamma p \to \pi X$ in the SLAC and Cornell high p_T, but very small ϵ regime is discussed in detail in Refs. 37,30. In these cases subprocesses giving the smallest powers of ϵ (e.g., $p + q \to \gamma + (qq)$ gives $(p_\perp^2 + m^2)^{-5}\ \epsilon^{0,1}$ rather than $\gamma q \to \gamma q$ which gives $(p_T^2 + m^2)^{-2}\ \epsilon^3$) are found to dominate and account for the data.

8. Charge-Cubed Test: The $e^\pm p \to e^\pm \gamma X$ Asymmetry

Even though deep inelastic Compton scattering is severely complicated by non-scale invariant background terms at small ϵ, this is not the case for the charge asymmetry measured in deep inelastic bremsstrahlung $e^\pm p \to e^\pm \gamma X$, which is sensitive to the scaling part of the virtual Compton amplitude. The cross section difference which is odd in the lepton charge, arises because of the interference between the Bethe-Heitler and Compton amplitudes and determines a discontinuity of $\langle p|J_\mu(x)\ J_\nu(y)\ J_\lambda(z)|p\rangle$. For the scaling region, with all invariants large, one has from the parton model[38]

$$\Delta\sigma(e^{\pm}p \to e^{\pm}\gamma X) = \sum_i Q_i^3 \, G_{q_i/p}(x) \, \Delta\sigma(eq \to e^{\pm}\gamma q)\big|_{s'=xs} \tag{8.1}$$

where

$$x = -q^2/2p\cdot q \,, \qquad\qquad q = p_e' + p_\gamma - p_e ,$$

and Q_i^3 is the cube of the parton charge. As shown in Ref. 38, the requirement of interference to create the $e^{\pm}$ asymmetry demands that only one quark line be active, and none of the background terms which contribute to deep inelastic Compton scattering occur. An analysis leading to the same conclusions based on a light expansion is given by J. Kiskis.[39] We note that the structure function $V(x) = \sum_i Q_i^3 G_{q_i/p}(x)$ has special properties. Since $V(x)$ is odd charge conjugation, the Pomeron and other even trajectories do not contribute and the distribution should exhibit a quasi-elastic peak at $x \sim 1/3$, characteristic of the valence quarks. Further, since $\sum_i Q_i^3$ can be related linearly to the total charge and baryon number of the target. $V(x)$ obeys an exact sum rule:

$$\int_0^1 V(x)\, dx = \sum Q_i^3 = \begin{cases} 5/9 & \text{(quark model)} \\ 1 & \text{(Drell-Yan-Levy-type integer charges)} \end{cases} \tag{8.2}$$

in the case of a proton target.

Recently, a Santa Barbara group[10] has successfully measured the asymmetry in a double arm experiment at SLAC. Although the asymmetry in the $e^{\pm}p \to e^{\pm}X$ monitor was negligible ($< 0.03\%$), the asymmetry became as large as 20-30% when the large p_T photon was observed. The measurements were consistent with the form of $\Delta\sigma$ predicted by the parton model, including the quasi-elastic peak. A preliminary analysis gives $\sum_i Q_i^3 = 0.88 \pm 0.44$, with the error limited by low statistics. Clearly it is important that these measurements be extended.

There are also very interesting hadronic charge asymmetries which can be measured in e^+e^- collisions

$$\Delta\sigma(e^+e^- \to \gamma + H^\pm + X)$$

$$\Delta\sigma(e^+e^- \to H^\pm\, e^+e^- X)$$

in annihilation and the two photon process, respectively. These also measure valence-dominated odd C structure functions and the parton charges cubed. A complete analysis of these processes is in preparation.[41]

9. Quasi-Elastic Peak in Inclusive Hadronic Reactions[30]

One of the most sensitive tests of the dynamics of the parton model is the measurement of differences in particle production, especially $d\sigma(pp \to K^+X) - d\sigma(pp \to K^-X)$, which is sensitive to the flow of the valence quantum numbers of the beam to the produced particle. For orientation, we begin by considering the trivial case when the binding of the hadrons A, B, C, vanishes. For equal quark masses, then $G_{a/A}(x) = \delta(x-n_a/n_A)$, $G_{b/B}(x) = \delta(x-n_b/n_B)$ in Eq. (2.1) where n_a is the number of quarks in a, $n_A = n_a + n_{\bar{A}a}$, etc. At 90°, we have

$$x_T^c = \frac{2}{x_a^{-1} + x_b^{-1}} = \frac{2}{\frac{n_A}{n_a} + \frac{n_B}{n_b}} \equiv \hat{x}_T^1 \qquad (9.1)$$

(This is multiplied by $x_C = n_C/(n_C + n_{\bar{C}c})$ if c fragments to C.) Turning on the binding we expect $\delta(x_T - \hat{x}_T^1)$ to spread out to a distribution in x_T which still remains peaked at the value $\hat{x}_T^1$. Since the cross section is parametrized as $\epsilon^{F_{eff}} = (1 - x_T)^{F_{eff}}$, we should then find $F_{eff} = 0$ at $x_T = \hat{x}_T^1$. More realistically, we know that the small x behavior of $G_{a/A}(x)$ diverges at $x \to 0$ due the presence of infinite number of partons in the Fock wave function of hadron A. A convenient parametrization is[30]

$$G_{a/A}(x) \propto (1 - x)^{2n_0(\bar{a}A)-1} x^{2n_a - 1} \sum_{\delta=0}^{\infty} \frac{[\lambda(1-x)^3 \log \frac{1}{x}]^\delta}{\delta!} \tag{9.2}$$

where each component

(a) obeys the spectator rule (3.5) for $n_0(\bar{a}A) + 2\delta$ spectators,

(b) peaks at $x = n_a/(n_0(\bar{a}A) + 2\delta)$,

and where the infinite sum converges to

$$G_{a/A}(x) \sim \frac{(1-x)^{g_a}}{x^{\alpha_A}} \qquad [x \to 1 \text{ or } x \to 0] \tag{9.3}$$

where $g_a = 2n_0(\bar{a}A) - 1$ and $\alpha_A = \lambda + 1 - 2n_a$.

Substituting (9.3) into (2.1) gives a form $(x_1 = -u/s$, $x_2 = -t/s)$

$$E \frac{d\sigma}{d^3p} \sim (p_T^2 + m^2)^{2-n_{active}} {}_\epsilon F \; x_1^{1-\alpha_A} \, x_2^{1-\alpha_B} \tag{9.4}$$

times a slowly varying function of x_1 and x_2. ($x_1 = x_2 = x_T/2$ at 90°.) Thus for $\alpha_A = \alpha_B = 1$ (Pomeron, Feynman scaling behavior) $F_{eff} \cong F$, and there is no quasi-elastic peak. Intuitively this corresponds to having n_A, $n_B \to \infty$ (unlimited number of spectators and $\hat{x}_T \to 0$ in Eq. (9.1). However, for processes sensitive to the quantum numbers of the beam, $\alpha < 1$, and we must have a quasi-elastic peak. The data for the difference of p and $\bar{p}$ and $K^+ - K^-$ production does seem to show a zero in the F_{eff} plot (see Fig. 8) at $x_T \sim 0.2$ to 0.3 at FNAL

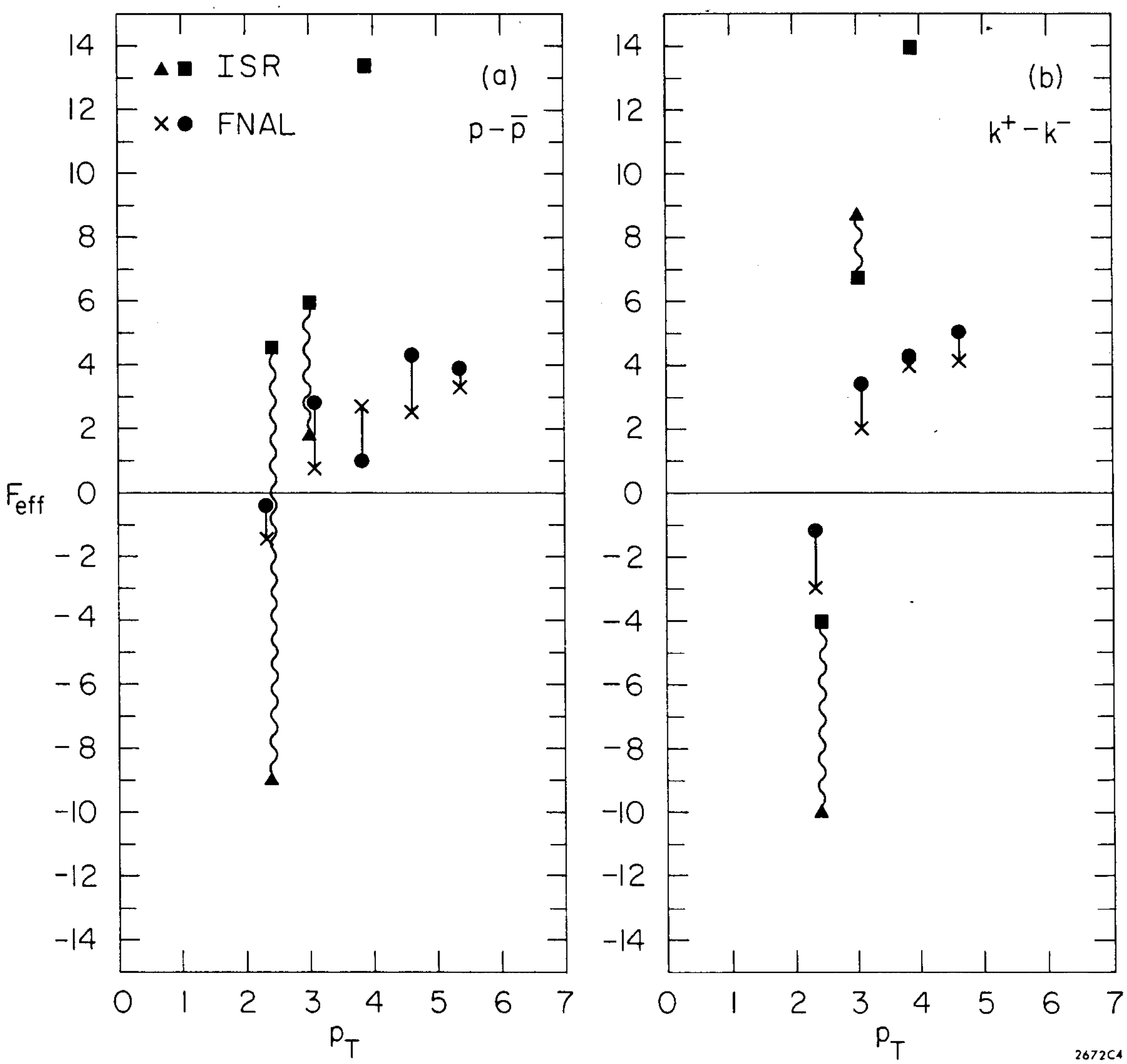

Figure 8. The extraction of F_{eff} for the difference of the p and $\bar{p}$ production cross sections and the difference of the K^+ and K^- production cross sections at the ISR (BS Collaboration) and FNAL (CP Collaboration). The points are labelled as in Fig. 7. A zero value for F_{eff} indicates a quasi-elastic peak in the ϵ distribution.

and $x_T \sim 0.1$ to 0.15 at the ISR ($K^+ - K^-$). The values are in reasonable agreement with the number of spectators expected in the CIM (see Ref. 30). In particular, roughly 1/5 to 1/3 of the incident beam momentum is found on valence partons for the FNAL kinematic range, and this is reduced by perhaps a factor of 2 in the ISR range, as expected from the increased number of spectators in the terms that dominate at large ϵ. This effective valence-momentum fraction is possibly useful as a guide to the relative effectiveness of proton beam energy compared to e^+e^- beams. Much more experimental data involving production particle and beam target particle differences and theoretical work will be required to fully exploit the important information in the parton distribution functions. It should also be interesting to correlate multiplicity in the fragmentation regions with the corresponding number of predicted quark spectators.

10. Correlations

Thus far we have discussed tests which only prove the short distance structure of the parton model. Detailed predictions for multiplicity distributions and correlations (quantum numbers, two multiparticle momentum distributions, etc.) involve the large distance properties of the theory--how the quark and simple hadronic states created in the irreducible subprocesses and the spectators evolve into physical hadrons. By making simplifying assumptions, many predictions can be made, but in most cases direct tests of the structure of the short distance quark mechanisms are not involved.

Bjorken[1] has already discussed the evidence for jet structure which is expected in any hard-scattering models based on two body reaction. We note that in the CIM the transverse momentum distribution away from the jet axis is always of the form of a sum of inverse powers, rather than the usually assumed exponential tail. For each contributing CIM subprocess one can predict where in phase space the conserved quantum numbers (B, Q, S) tend to distribute when a large p_T particle is detected (making the usual assumptions on quantum retention of the partons). Thus where $q + (qq) \to M + B$ is the important subprocess, a baryonic system is expected to recoil against a meson trigger. In K^+ production, strangeness is typically balanced in the beam fragmentation region. On the other hand in K^- production, strangeness should be balanced locally. Other examples are discussed in Refs. 30 and 42.

Many aspects of the angular correlations expected in the CIM are discussed by Raitio and Ringland[42] and in Ringland's[43] contribution to this conference. I will only briefly discuss one aspect of the correlations here. A useful formula for understanding the momentum balance in a large p_T reaction is the purely kinematic relation

$$\cot \theta_d = \cot \theta_c \pm \left(\frac{x_a - x_b}{x_T}\right) x_C \tag{10.1}$$

where the cm angles are measured with respect to the beam; $\theta_d = \theta_c$ is "back to back." The important values of x_a, x_b and x_C are controlled by the G distributions and the weight of the cross section $d\sigma/dt'(a + b \to c + d)$. We note that

(a) The jet along d will be back to back with the jet along c ($\theta_c \cong \theta_d$) if $\langle x_C\rangle/x_T$ is small and/or $\langle x_a - x_b\rangle$ is small. Note that on the average $\langle x_c\rangle$ is smaller for pions than for other hadrons since the pions can be daughters or decay products.

(b) Conversely, the divergence from back-to-back jets is increased if $\langle x_a - x_b \rangle$ is peaked at a large value (as is characteristic of CIM processes with $a \neq b$).

(c) For $\theta_c = 90^\circ$, Eq. (10.1) gives a smeared double peak solution for θ_d which becomes flattened or peaks toward $\theta_d = 90^\circ$ in order to minimize s'.

(d) For $\theta_c < 90^\circ$, there are two peaks in θ_d, with the one tending toward the same direction as θ_c dominanting to minimize s'. The situation is further complicated if $d\sigma/dt'(a + b \rightarrow c + d)$ has strong t' or u' dependence.

Comparisons with present data are sometimes treacherous since one has to rely on somewhat uncertain peaking of multiplicity distributions which are also subject to normalization uncertainties.

The theoretical predictions for momentum balance can be most readily compared with data where the momenta of the particles in the recoil system are measured. Extensive calculations are now in progress which utilize the full $G_{a/A}(x,K_\perp)$ distributions to generate events in a Monte-Carlo program.[44] More sensitive tests will also require quantum numbers of the leading particles in the jet system. It is also particularly interesting to measure difference in correlations when the trigger is p vs. $\bar{p}$ or K^+ vs. K^-, since the valence part of the distribution functions must be involved.

A possible difficulty for the CIM, as emphasized by Contogouris and Schiff[45] are the correlations between high particles produced at 90° on opposite sides. If the dominant process for $pp \rightarrow \pi_1\pi_2X$ is $qM \rightarrow q'\pi_1$, with $q' \rightarrow \pi_2 + q''$, then there should be a cross section minimum at $p_\perp^{(2)} = p_\perp^{(1)}$. This is not evident in the present data for $x_T^{(1)} \sim 0.15$. However, the meson produced in the CIM process $q + M \rightarrow q + M$ is a minimal or "bare" meson state consisting of two hard quark partons. Unless it is limited by kinematics, such a state can continue to evolve into a physical meson state by radiating slow hadrons--just as a bare electron produced in the final state must create its electromagnetic self-field to form a physical electron. Thus it is probably unlikely that a detailed pion can be identified universely with the meson state M. A further reduction of the minimization at $p_\perp^{(2)} = p_\perp^{(1)}$ also occurs if M is a decay product of a heavier hadron, e.g., a ρ or kaon. At low x_T one thus expects extra multiplicity and a positive correlation for a hadron to be emitted on the same side. However, for large $x_T^{(1)}$ where phase space is limited, it is unlikely that extra spectators are produced along the trigger and the $qM \rightarrow qM$ subprocesses should yield a minimum at $p_\perp^{(2)} = p_\perp^{(1)}$. Note, however other contributing processes like $q + q \rightarrow \pi^+ + \pi^-$ and $q + (qq) \rightarrow \pi + B$ have maxima at $p_\perp^{(2)} \simeq p_\perp^{(1)}$.

11. The Multiplicity Bump at Large p_T

It is often stated that no sharp change is evident in data which unequivocally indicates the on-set of new physics at large p_T. However, the Argo spectrometer group of E. W. Anderson et al.[46] at BNL did find that for fixed $\mathcal{M}^2$, the changed multiplicity measured in the inclusive reactions $pp \rightarrow pX$ and $pp \rightarrow \pi X$ at $p_\perp = 28.5$ Gev/c shows a change of $\Delta n_c \sim 1$ over an interval in $p_T \sim 0.7$ to 1.0 Gev/c which moves in with increasing $\mathcal{M}^2$ (see Fig. 9). It would seem to be difficult to explain this result in terms of extended Regge, eikonal,

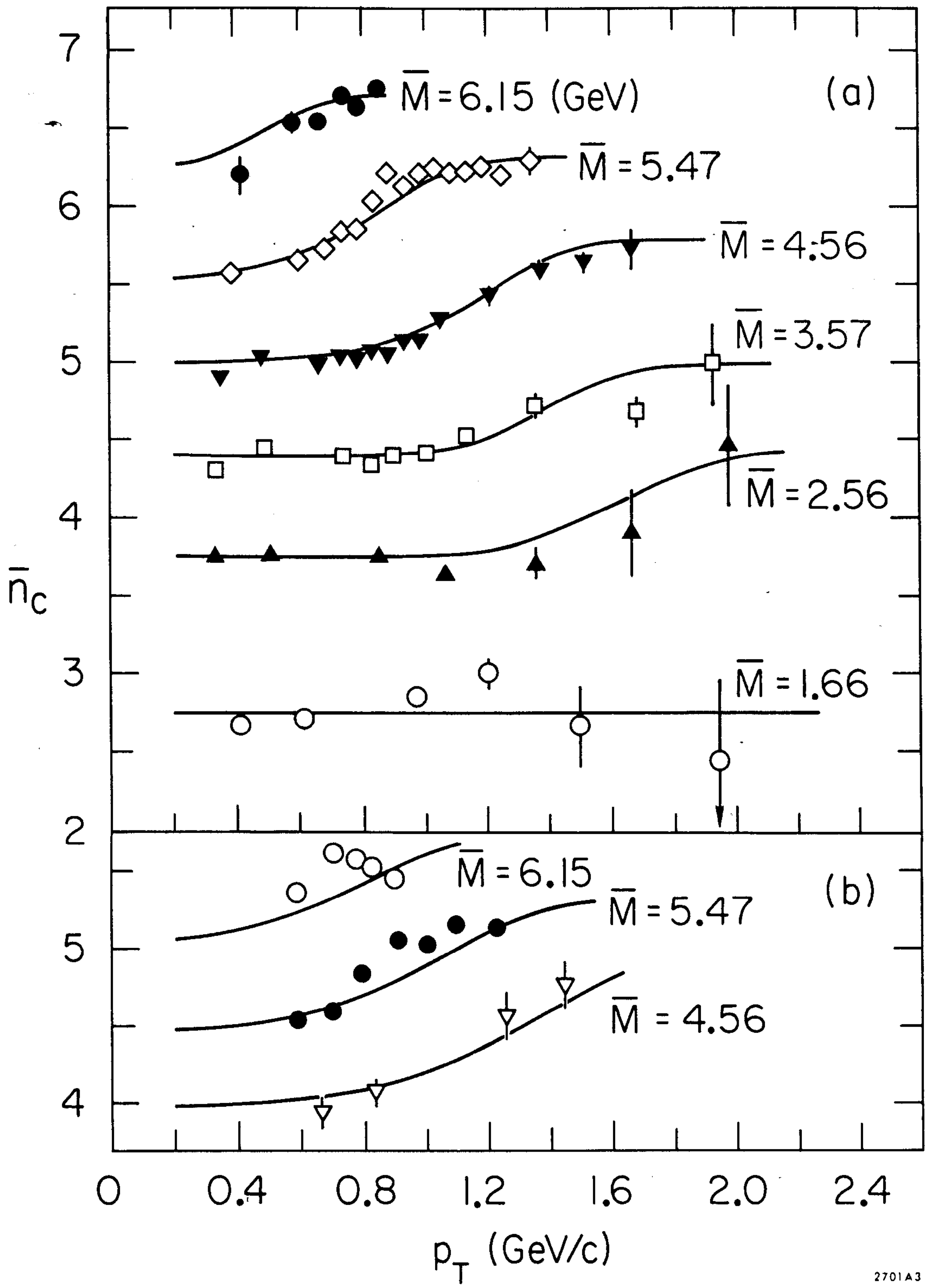

Figure 9. Multiplicity bump in the Argo data.[46] [From Alonso and Wright, ref. 47.]

or statistical models, without introducing new thresholds, etc.

In a recent paper, Alonso and Wright[47] have shown that the Argo data can be explained simply in terms of the existence of two components in the inclusive cross section:

(a) A soft component $\exp(-6p_T^2)$ with the usual Regge parameterization and an associated multiplicity

$$\bar{n}_s \sim 2 + \log \mathcal{M}^2 , \qquad \text{(Gev units)} \qquad (11.1)$$

(b) A hard component (consistent with the CIM) of the form of a sum of terms $\sum(p_T^2 + m^2)^{-n} (1-x_R)^F$ fitted to the large p_T data, with an associated multiplicity

$$\bar{n}_H \sim 2.7 + 0.5p_T + \log(\sqrt{s} - \sqrt{s'})^2 \qquad (11.2)$$

which agrees with the ISR multiplicities. The last term accounts for the spectator multiplicity. The sum of contributions agrees with the Argo data (see Fig. 9). Further tests involving other energies, angles, and other beams (meson, photon) are clearly necessary to confirm this hard-scattering model explanation. A related discussion, based on the hadronic bremsstrahlung picture of Ref. 48 has also recently been given by Gutay et al.[49]

12. The Partition Method for Bound State Calculations

There are many methods available for obtaining the covariant amplitude for processes involving the scattering of hadrons. These include Bethe-Salpeter methods, Fock space calcuations in time-ordered perturbation theory, Sudakov analyses, etc. Perhaps the simplest method is the "partition" method discussed in Ref. 5, which is particularly convenient for analyzing scaling behavior of amplitudes, and also for proving cancellations in the infrared region. In general, one replaces each hadron by a cluster of constituents, where each particle has a finite fraction of the hadron momentum: $(p^{(+)} \equiv p^0 + p^3)$

$$\begin{aligned} p_i^{(+)} &= x_i p^{(+)}, & \sum x_i &= 1, \qquad 0 < x_i < 1 \\ \vec{p}_{\perp i} &= \vec{\kappa}_{\perp i}\ , & \sum \vec{\kappa}_{\perp i} &= \vec{p}_\perp = 0 \end{aligned} \tag{12.1}$$

In general, the hadronic wave function controls the relative probability for a given number of constituents and the convergence of the x_i and $\vec{\kappa}_{\perp i}$ spectrum. Note that in the zero binding limit we must have

$$\left.\begin{aligned} x_i &\to m_i/M \\ \vec{\kappa}_{\perp i} &\to 0 \end{aligned}\right\} \text{B.E.} \to 0\ . \tag{12.2}$$

Further, in the limit of small interaction strength only the minimally-connected graphs would be important.

We now make the following ansatz: The short distance behavior and fixed angle scaling properties of hadronic amplitudes are independent of the magnitude of the hadronic binding. In this case the leading asymptotic behavior is identical to that obtained by partitioning each hadron's momentum among its constituents and calculating the minimal connected graphs (including the usual spinor factors). Examples are shown in Fig. 10.for the nucleon form factor and $K^+p \to K^+p$ amplitude.

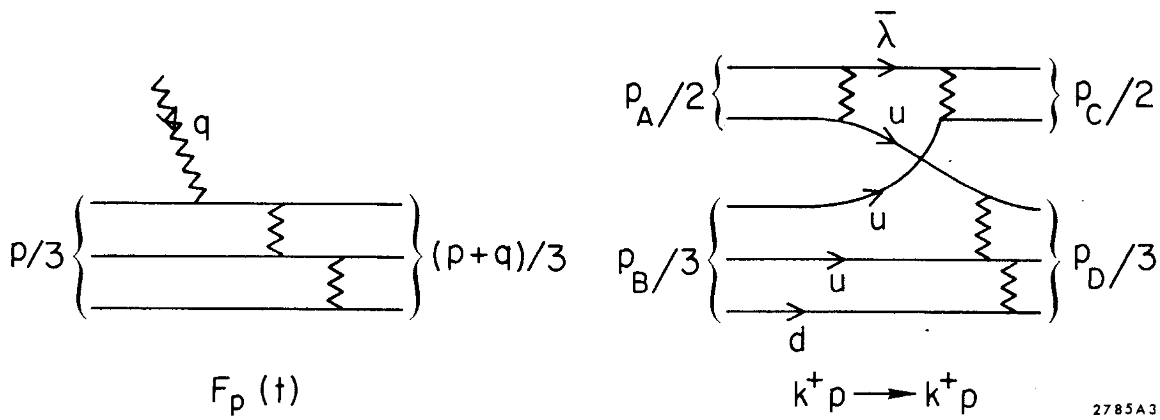

Figure 10. Partition graphs for $F_p(t)$ and $K^+p \rightarrow K^+p$.

The interaction kernel is iterated wherever large momentum transfer is involved. In general all possible routings are required. The important graphs of the CIM are reviewed in Section 15.

Since the calculations do not include loops, they are extremely simple. In the case of renormalizable theories, the gluon couplings always cancel its propagator in the scaling behavior so (after spin projection) only the quark propagator k^{-2} contributes to the fall-off. It is then simple to verify the dimensional counting rule $F(t) \sim t^{-n+1}$ for the spin-averaged form factor and $\mathcal{M}(K^+p \to K^+p) \sim u^{-1}t^{-2}$, for Fig. 10, and the general fixed-angle scaling result $\mathcal{M}_n \sim (\sqrt{s})^{4-n}$, $n = n_{active}$, independent of constituent spin. It is also easy to see that the partition model is always gauge invariant as long as all possible photon insertions are made along each charged line.

13. Proofs of Dimensional Counting

The technical condition for the minimally-connected partition graphs to give the correct asymptotic behavior is the finiteness of the Bethe-Salpeter wave-function at the origin (since in this case further iterations of the Bethe-Salpeter kernel lead to non-leading contributions). Non s-states are discussed in Ref. 5. In asymptotic freedom theories one can show--at least in non-gauge models--that this condition is satisfied up to calculable corrections involving a finite power of logarithms.[53] In the case of gauge theories the fact that hadron has total zero charge (color singlet) with respect to gluon coupling leads to a cancellation of all infrared singularities for hadronic matrix elements. This is shown explicitly for the Abelian and non-Abelian cases in Ref. 5 and

50 , respectively. In the case of color models we also note the following: Emission of a color octet from an external color singlet hadron requires a color octet intermediate state. As long as $m_8^2 - m_1^2 \neq 0$, the vanishing of the energy denominator at $k^\mu \to 0$ necessary for an infrared singularity in the gluon momentum cannot occur. Thus the extra complications of the gauge theories do not affect the hadronic scaling laws. Note that the partition method always give the correct scaling law in the limit of small coupling strength and binding and thus even in a theory with wave function anomalous behavior gives an important constraint on calculations.

Important progress has also been made on the contributions of pinch singularities of the type discussed by Landshoff.[51] Note that in the case of graphs involving multiple quark-quark scattering between quarks of different hadrons, the intermediate states can be on-shell leading to singularities in the x_i integrations. The amplitude at the singularity essentially becomes the product of independent near-on-shell quark-quark scattering amplitudes. As has often been noted, such graphs do not occur by hypothesis in the CIM because of the requirement of quark exchange or interchange. Further, since scale-invariant quark-quark interactions are not seen in inclusive large p_T reactions, these pinch contributions presumably are unimportant on phenomenological grounds.

However, it now appears that even, in principle, such contributions do not occur in leading order of the power-law scaling in gauge theories. Cornwall and Tiktopoulous[50] have shown that, because the pinch contribution is proportional to a disconnected $t \neq 0$ quark-quark scattering amplitude, an infrared factor of the form $\exp(-g^2 \log^2 t/\lambda^2)$ automatically damps the amplitude faster than any power. The possible existence of such a mechanism was originally suggested by Polkinghorne[52] and by Appelquist and Poggio.[53] The parameter λ^2 is a measure of how far the quark is off-shell and thus is proportional to the binding energy $\lambda^2 \sim (B.E.)m$, and the Landshoff contribution vanishes rapidly as the $B.E. \to 0$.

We should also comment here that the dimensional counting rules can be derived in a more formal fashion for scale-invariant theories using a short-distance expansion of the Bethe-Salpeter wave function. This is straightforward in the case of spinless constituents, but is more subtle in the case of spin.[54] An elegant discussion and references to earlier work is given by Polyakov in his report to the SLAC Symposium.[55] As shown in Ref. 6, the spin complications occur because the important part of the wave function (which controls the convergence of the partition diagrams) is actually the coefficient of the "on-shell" spinors in Salpeter's[56] expansion of the wave function: e.g. for the pion

$$\psi_{BS}(p) \sim u(p_1)\ v(p_2)\ \psi_{++}(p) + \cdots \tag{13.1}$$

The spinors are included in the definition of partition amplitude. The $\psi_{++}(p)$ wave function has the same dimension and scaling properties as the spinless theory.

14. Minimal Neutralization and Quark-Quark Scattering

A central and recurring problem in the understanding of large p_T inclusive reactions is the phenomenological absence of scale-invariant quark-quark interactions. In the CIM the absence of such an interaction is a postulate; quarks only interact within the confines of the hadronic "bag" and only quark-hadron scattering kernels occur. This is also equivalent to the basic duality argument that all intermediate states must conform to the composition and quantum numbers of the observed hadrons. The presumed absence of hadronic states with a <u>hard</u> gluon constituent negates the importance of a hard gluon exchange contribution.[57]

Another possible reason occurs in the context of color models. In order to prevent the emission of states with non-zero color, gluon exchange requires that at minimum two vacuum quark lines arise to neutralize all the quantum numbers of the final state (see Fig. 11). On the other hand, e^+e^- annihilation (via $e^+e^- \to q\bar{q}$), deep inelastic scattering $(eq \to eq)$, the Drell-Yan process $(q\bar{q} \to \mu^+\mu^-)$, and essentially all the CIM processes $(q\bar{q} \to M\bar{M},\ qM \to qM,\ q(qq) \to MB,$ etc.) require only <u>one</u> quark line neutralization. The sole exception is the mechanism $qq \to B\bar{q}$, which again requires two-line neutralization. In fact, fits to $pp \to pX$ do not demand the presence of this mechanism. It is thus conceivable that there is a dynamical reason for minimal neutralization (and in turn minimum multiplicity) in a high energy collision.

In any event, regardless of the eventual importance of a gluon exchange contribution, the quark exchange and interchange contributions are not suppressed in any parton model, and must be taken into account.

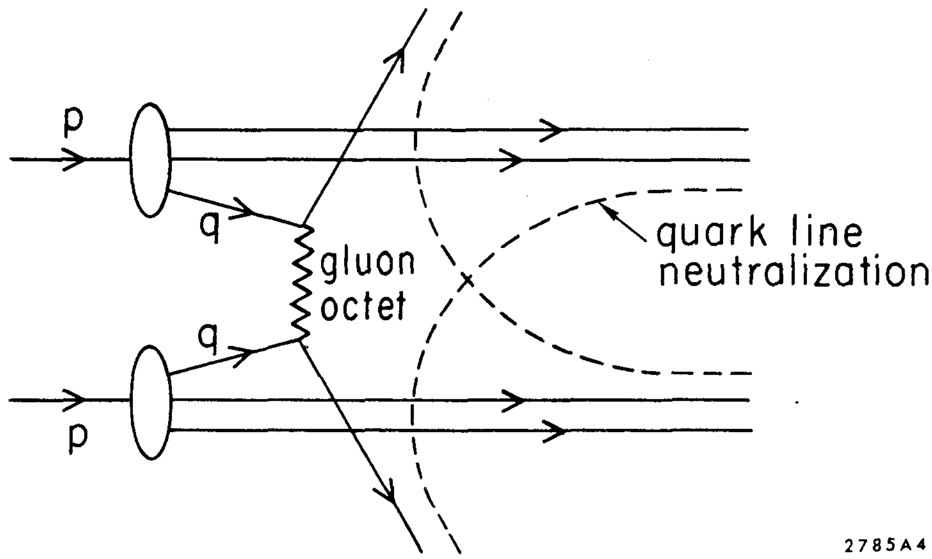

Figure 11. Double quark line neutralization (dashed line) required for a gluon exchange contribution, to $p + p \to \pi + X$.

15. Development of the Constituent Interchange Model[4]

There are many ways to motivate the hypothesis that quark exchange and interchange is the dominant hadronic interaction at short distances. The interchange model gives a dynamical, covariant realization of duality diagrams for exclusive processes at large t and u. It thus automatically satisfies the constraints of analyticity, crossing behavior, and leads to a smooth connection to the usual Regge physics of small t and u. In particular, if an amplitude is exotic in the s-channel (e.g. $K^+p \to K^+p$), the amplitude continues to be exotic at large θ_{cm}.[59]

The interchange model can also be motivated directly from the parton model starting from the usual "handbag" diagram for deep inelastic processes (see Fig. 12a). The same diagram (plus the crossed graph) gives a contribution to Compton scattering of the form

$$\begin{aligned} \frac{d\sigma}{dt}(\gamma p \to \gamma p) &\sim F_p^{(+)2}(t)\, \frac{d\sigma}{dt}(\gamma q \to \gamma q) \\ &\sim 4\pi\alpha^2 \frac{F_p^{(+)2}(t)}{s^2}\,[1 + O(t/s)] \end{aligned} \tag{15.1}$$

which corresponds to a $j = 0$ fixed pole contribution at $s \gg t$,[60] and s^{-6} behavior at fixed angle--assuming, as is true from dimensional counting, that $F_p^{(+)}(t)$ (which is an even C nucleon form factor) falls as t^{-2}. [This result can easily be extended to give usual Regge behavior at small t via the choice of the x-distribution; see ref. 48.]

If we replace one photon by a meson then we obtain immediately the interchange model for meson photoproduction--basically impulse approximation

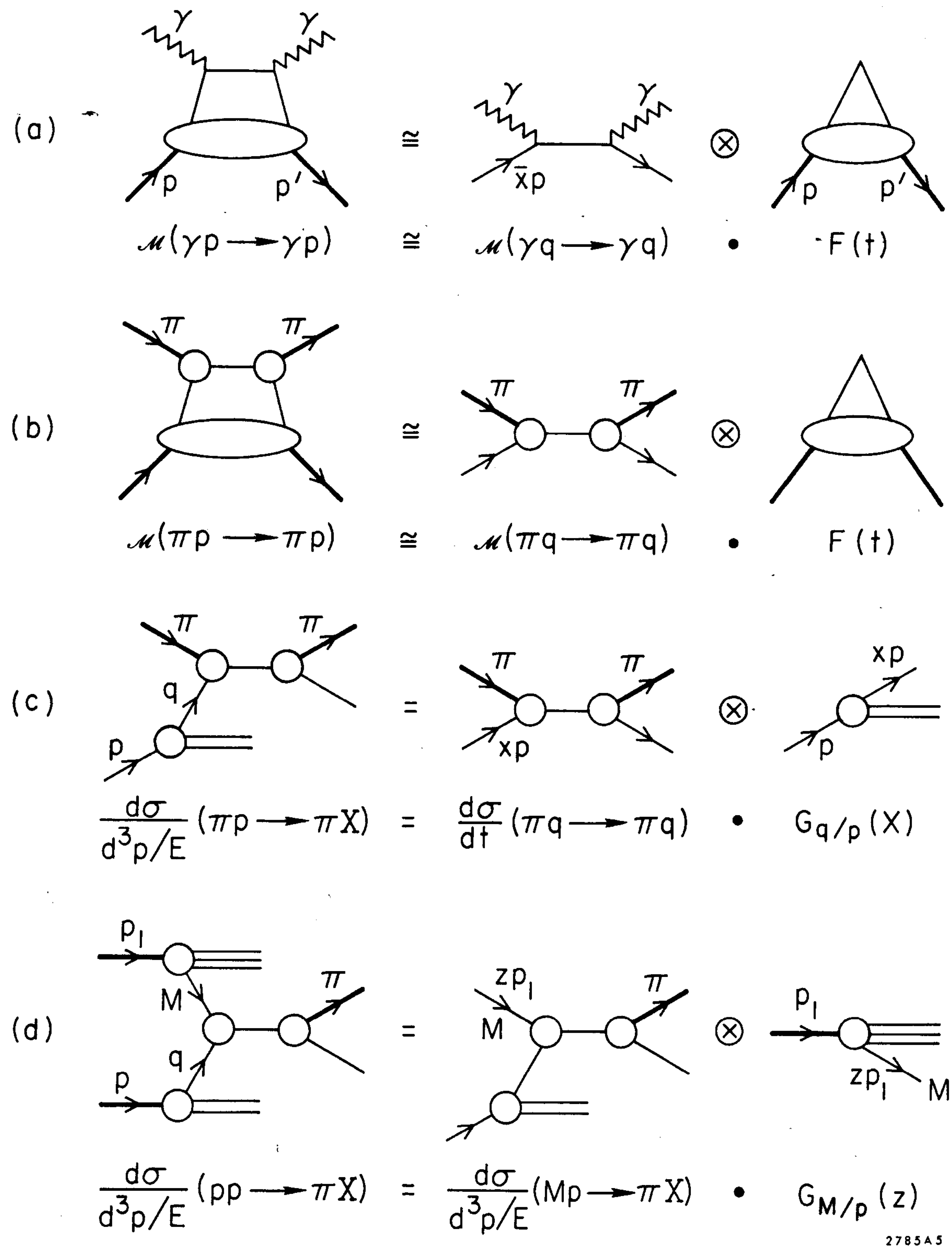

Figure 12. Inductive derivation of the CIM (see text).

$$\frac{d\sigma}{dt}\,(\gamma p \to \pi p) \sim F_p^2(t)\,\frac{d\sigma}{dt}\,(\gamma p \to \pi p)$$

$$\sim s^{-7}\, f(\theta_{cm}) \qquad (15.2)$$

The scaling behavior holds provided $F_\pi \sim t^{-1}$. Similarly, replacing the other photon vertex by a Bethe-Salpeter bound state, we obtain a model for meson-baryon scattering at large t and u (see Fig. 12b):

$$\frac{d\sigma}{dt}\,(\pi p \to \pi p) \sim F_p^2(t)\,\frac{d\sigma}{dt}\,(\pi q \to \pi q)(-\frac{u}{s})$$

$$\sim s^{-8}\, f(\theta_{cm}) \qquad (15.3)$$

This connects for $s \gg -t \gg m^2$ to the asymptotic Regge behavior $\mathcal{M} \sim s^{-\alpha(t)}\beta(t)$ with

$$\alpha(t) \to -1, \quad \beta(t) \to t^{-2} \qquad \text{at large } t\,. \qquad (15.4)$$

[The factor $(-u/s)$ corresponds to dominance of the helicity conserving amplitude.] Again we remark that the meson-nucleon amplitude has the same analytic and exoticity structure as duality diagrams. For the case of $K^+p \to K^+p$ we have $\mathcal{M} \to u^{-1}F_p(t)$, with discontinuities only in u and t. A comparison with the data for K^+p and K^-p scattering is given in refs. 3, 23.

Continuing inductively, we can obviously obtain a contribution to inclusive meson nucleon scattering by opening up the quark line as in Fig. 12c. This immediately gives in analogy with $ep \to eX$

$$\frac{d\sigma}{dt\,dx}\,(\pi p \to \pi X) = \frac{F_2(x)}{x}\,\frac{d\sigma}{dt}\,(\pi q + \pi q) \qquad (15.5)$$

where the quark carries fractional momentum

$$x = x_{BJ} = \frac{K_0 + K_3}{p_0 + p_3} = \frac{-t}{\mathcal{M}^2 - t} \tag{15.6}$$

This gives a contribution [4]

$$\frac{d\sigma}{d^3p/E}(\pi p \to \pi X) \sim \frac{x_T^2}{p_T^8}(1 - x_T)^3 \tag{15.7}$$

with the scale set by the scaling of the $qM \to qM$ amplitude. The contribution (15.7) clearly satisfies the exclusive-inclusive connection to (15.3) and automatically extends the usual formulae for the triple Regge region. This contribution is however not important in the central region at small x_T. In a general inclusive process-away from the edge of phase space--there will be radiation, i.e., hadronic bremsstrahlung from all the external lines. The beam, target, and produced particles each radiate energy along the momentum direction producing extra spectators. (Note that $F_2(x)$ already includes target bremsstrahlung.) We thus obtain the contribution of Fig. 12d, and a contribution of the general form (2.1) where the active subprocess is $Mq \to Mq$, and M is a virtual $(q\bar{q})$ state with the quantum numbers of a meson. Thus, in general, the CIM leads to Eq. (2.1) where the active subprocess is any amplitude involving hadron scattering or production. The inductive argument given here shows that neither gluon interactions nor the scattering of quarks of different hadrons need be considered explicitly.

16. The A Dependence of High p_T Reactions

One of the most fascinating aspects of high p_T reactions--especially from the standpoint of the quark parton model--is the question of nuclear target effects. Among the general questions involved are the nature of shadowing effects, the possibility of coherent and multi-nucleon reactions, the different nature of interactions of soft and hard partons, and the influence of the nuclear environment on quark confinement and quantum number neutralization.

(a) Inclusive Reactions: The $p_L = 300$ Gev/c FNAL-CP data[11] for $pA \to HX$ near 90^o depends on nuclear number as $A^{n_H(p_T)}$, where for $p_\perp \sim 4$ to 6 Gev/c, $n_\pi \sim 1.1$, $n_{K^+} \sim 1.2$, $n_{K^-} \sim n_p \sim n_{\bar{p}} \sim 1.3$. The fact that n_H is not below 1 apparently indicates that each nucleon of the target participates in the reactions, and thus there is no absorption of the hard partons initiating the high p_T reactions. Further, $n_H > 1$ indicates either a collective multinuclear effect[61] or a multiple scattering mechanism.[62] The former explanation (although in principle possible for CIM mechanisms like $q + q + \to M + \bar{B}$, or Landshoff-type diagrams) would require coherence of quark amplitudes over large nuclear distances. Futhermore, the form of the A dependence is not naturally fit using a linear combination of terms, A, A^2, A^3.[62]

The more conventional solution, based on a careful analysis of double-scattering processes has been offered by J. Kuhn.[62] He assumes the single nucleon cross section has a two component form fitted to ISR data where the hard shadowing term (being due to the interactions of hard parton components of the beam) is unshadowed (proportioned to A) and the "soft" component (which arises due to the usual peripheral, diffractive dissociation of the beam, i.e., wee-parton interactions) has the same A dependence as the total cross section ($\propto A^{0.85}$). In addition, states produced (at moderate p_T) by the hard component can traverse the nucleus and interact again with another hard interaction $H + p_2 \to \pi + X_2$ to produce the final observed hadron at large p_T. (This "secondary beam" is assumed not to be shadowed, since it mainly consists of hard partons and there is insufficient time to develop a completely dressed hadron.) The double-scattering term gives an $A^{4/3}$ contribution. Kuhn finds that the observed A dependence of $pA \to \pi X$ can be reproduced using this model. [See Figure 13.] Kuhn's explanation, however, demands that the second hard scattering $(q\bar{q}) + p' \to \pi + X_2$ has a relatively slow fall-off $\sim (p_\perp + m^2)^{-4}\epsilon^3$, as suggested by the CIM, in the required small ϵ, high p_T forward angle region of the Peyrou plot. Further tests of Kuhn's model are clearly required, especially the predicted energy and angular dependence on A, as well as predictions for different particle types. Note that the CIM would predict less double scattering for $\pi A \to \pi X$ since there is relatively less advantage in using the hard component twice.

If the double-scattering explanation is correct, then there are also obvious consequences for the structure and multiplicity of the associated nuclear recoil system $X_1 + X_2$, coplanarity distributions, etc.

(b) Lepton Processes: The standard tests of the quark parton model, when performed on a nuclear target, can yield further essential information on the internal hadronic mechanisms. If hard partons are not absorbed then clearly no shadowing ($\sigma \propto A$) is expected for the scaling contributions to $eA \to eX$, $pA \to \mu^+\mu^- X$ at large x. Both experiments also

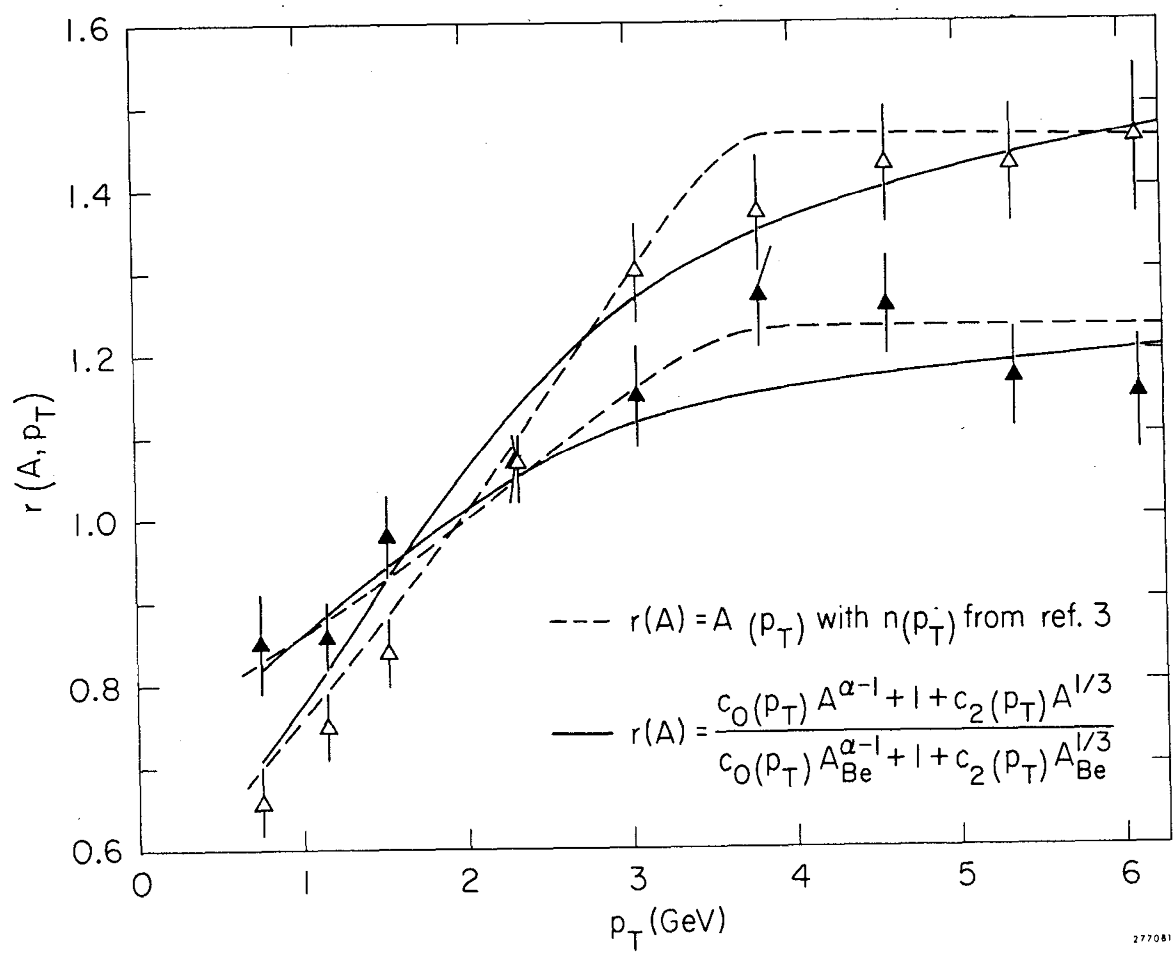

Figure 13. A dependence of the FNAL-CP data[11] at p_{Lab} = 300 GeV/c, and Kuhn's calculation (solid line). From J. Kuhn, ref. 62.

can test the nature of $G_{q/A}(x)$ at small x and the possibility of shadowing and antishadowing, as predicted by Nicolaev and Zakharov.[63] An alternative view is discussed in Ref. 64.

It is also particularly interesting to study the A dependence of the reaction $eA \to eHX$ in the photon fragmentation region, in order to see how the nuclear environment influences the kinematic dependence of the fragmentation function $G_{H/q}(x,\vec{k}_\perp)$. Furthermore, particle ratios at high p_T might be sensitive to changes in the quark-neutralization process induced by the nuclear medium.[65]

(c) Elastic Scattering: Another intriguing possibility is that there is no shadowing in quasi-exclusive asymptotic wide-angle scattering processes. If we argue that only the hard-parton constituent states of the beam are effective in initiating a large angle scattering process, then no shadowing for these components implies[66]

$$\sum_{A'} \frac{d\sigma}{dt}\,(HA \to HA') \to Z\,\frac{d\sigma}{dt}\,(Hp \to Hp) + (A-Z)\,\frac{d\sigma}{dt}\,(Hn \to Hn) \tag{16.1}$$

at large t and u. The allowed final state in the quasi-exclusive scattering consists of any excited nuclear state A' including nucleon recoil without any extra hadrons being produced. Note that Fermi-motion corrections normalize out at large p_T, and double-scattering contributions should not be important in the power law region.

We emphasize that the underlying assumption for the validity of (16.1) is that the parton-Fock space of the incident hadron has a non-zero probability for a state with only hard parton constituents. Due to their small interaction size, such partons are assumed to completely penetrate the nucleus. In addition to resolving the validity of these intriguing assumptions, the phenomenology of quasi-exclusive nuclear scattering could also be very interesting. For example, if Eq. (16.1) is correct, then the CIM predicts

$$\sum_{A'} \frac{d\sigma}{dt} (K^+A \to K^+A') \to \frac{A+Z}{2} \frac{d\sigma}{dt} (K^+p \to K^+p) \ , \tag{16.2}$$

since only the up quarks in the nucleus participate in the interchange interaction. Thus extraordinary dependence on A and Z is a dramatic consequence of the quark model framework for large angle processes. We also note that measurements of (16.2) provide an increased rate for checks of fixed angle scaling at larger values of t and u.

A more general discussion of the material in this section will be given in Ref. 64.

Conclusions.

It is interesting to note that many of the postulates of the CIM and dimensional counting rules are natural features of quark models based on gauge field theories. The validity of the impulse approximation at large p_T can be connected with asymptotic freedom and the existence of Bjorken scaling. The dominance of quark exchange or interchange compared to single gluon exchange in exclusive processes is automatic in color models. Continuity with inclusive processes at fixed $\mathcal{M}^2$, or the minimum neutralization postulate may account for absence of gluon exchange in high p_T inclusive reactions. Furthermore, the work of Refs. 5 and 30 shows that the infrared complications of the vector theories are not operative in the case where the external states are all neutral (color singlets).

It is also striking that so many features of conventional quantum electrodynamics (form factors, fixed angle scattering of bound states, etc.) have the same behavior and satisfy the same counting laws which are now being observed in hadron physics--at least up to order α log s. (Compare, e.g., elastic $\pi - \pi$ and elastic positronium-positronium scattering.) The problem of untangling hadron dynamics is thus very much like unraveling the structure of quantum electrodynamics from the scattering and spectra of the leptonic bound states.

The CIM together with the dimensional counting rules are consistent with a) crossing symmetry; b) usual Regge forms (exclusive and inclusive) at small p_T; c) continuity throughout the Peyrou plot including the exclusive-inclusive connection; d) duality and the constraints of dual diagrams at large p_T; e) Bjorken scaling behavior and scale invariance at short distances; f) power law fall-off in all momentum transfer variables; g) a purely hadronic description of hadron scattering at small p_T. On the other hand, absorption, geometric effects, or consequences of quark confinement are not explicitly taken into account. Normalization cross checks between form factors, hadronic scattering amplitudes, structure functions, and decay rates--all of which are normalized to the Bethe-Salpeter wavefunction at the origin--have not yet been systematically applied. Further gauge-invariant calculations of photo and electroproduction amplitudes are also required.

It is apparent from the success of the quark counting rule for the deuteron form factor and the other nuclear effects discussed in Section 16 that the nucleus provides another testing ground of the quark model. The quark degrees of freedom become important for nuclear physics at momentum transfers beyond 1 Gev/c^2, and provide an important constraint on the asymptotic behavior of the nucleon interaction, exchange currents, and distribution functions. A number of predictions are discussed in Section 16.

Large p_T physics is still largely a phenomenological science, and a great number of experimental clues will be required for further progress. Among the most important tests of the quark-parton model are (a) further confirmation of jet structure; (b) scaling laws (p_T^{-4} ?) for jet + jet production at a given total p_T; (c) tests of scale-invariance and normalization of the Drell-Yan process $p + p \to \mu^+ \mu^- X$ or $p + p \to \mu + X$, and production of real and virtual photons at large p_T; (d) detailed single particle distributions on a proton target throughout the Peyrou plot; (e) large p_T production by photon, meson, anti-proton beams; (f) differences of particle/anti-particles in beam, target and projectile; (g) structure of complete events with a high p_T trigger; (h) correlations with momentum measurements and tracing of quantum numbers; (i) the production of new particles at large x_L or p_T. All of these measurements can lead us further to the goal of understanding the underlying dynamics and degrees of freedom of hadrons at short distances.

ACKNOWLEDGMENTS

The work on dimensional counting and the constituent interchange model is based on collaboration with Glennys Farrar, Dick Blankenbecler, and Jack Gunion. I am grateful to them and to J. Alonso, J. Bjorken, J. Kuhn, R. Raitio, G. Ringland, D. Sivers, D. Wright, and D.R. Yennie for discussions and helpful suggestions.

REFERENCES

1. J. D. Bjorken, Proc. of the Summer Institute on Particle Physics, SLAC (1975).

2. M. Davier, Proc. of the Summer Institute on Particle Physics, SLAC (1975).

3. D. Sivers, S.J. Brodsky, and R. Blankenbecler, SLAC-PUB-1595 (1975), to be published in Physics Reports.

4. J. F. Gunion, S. J. Brodsky, and R. Blankenbecler, Phys. Letters 39B, 649 (1972); Phys. Rev. D8, 287 (1973), Phys. Rev. D6, 2652 (1972), Phys. Letters 42B, 461 (1973).

   P.V. Landshoff and J.C. Polkinghorne, Phys. Rev. D8, 4157 (1973); Phys. Letters 45B, 361 (1973), preprint DAMTP 73/22(1973); Phys. Rev. D10, 891 (1974).

5. S. Brodsky and G. Farrar, Phys. Rev. Letters 31, 1153 (1973), Phys. Rev. D11, 1309 (1975).

6. V. Matveev, R. Muradyan, A. Tavkhelidze, Lett. al N.C. 7, 719 (1973).

7. R. Blankenbecler and S. J. Brodsky, Phys. Rev. D10, 2973 (1974); J.F. Gunion, Phys. Rev. D10, 242 (1974); R. Blankenbecler, S. Brodsky, J. Gunion, SLAC-PUB-1585 (1975) (to be published in Phys. Rev.).

8. S.M. Berman, J.D. Bjorken, J.B. Kogut, Phys. Rev. D4, 3388 (1971); J. Bjorken, Phys. Rev. D8, 4098 (1973). Other derivations of the hard scattering model are given in refs. 3, 4, and 7.

9. F.W. Busser, et al., Phys. Letters 46B, 471 (1963); J. A. Appel, et al., Phys. Rev. Letters 33, 419 (1974).

10. B. Alper, et al., Phys. Letters 47B, 75 (1973); Phys. Letters 47B, 275 (1973); Nucl. Phys. B87, 19 (1975); CERN preprint (1975); G. Jarlskog, Proc. Conf. on High Energy Hadronic Interactions, Recontre de Moriond 1975.

11. J.W. Cronin, et al., Phys. Rev. Letters 31, 1426 (1973), Chicago EFI preprints 74-1181 and 74-1182.

12. G. R. Farrar, Nucl. Phys. B77, 429 (1974); J. Gunion, ref. 4.

13. R. Blankenbecler and C. Sachrajda, SLAC-PUB-1658, 1975.

14. R. Blankenbecler, S. Brodsky and C. Sachrajda, in preparation.

15. V. N. Baier, V.S. Fadin and V.A. Khoze, Nucl. Phys. B65, 381 (1973).

16. M.S. Chen and P. Zerwas, Phys. Rev. D11, 58 (1975), and references therein.

17. Z.F. Ezawa, N.C. 23A, 271 (1974).

18. G. Farrar, Caltech preprint (1975).

19. D. Sivers, Ann. Phys. (NY) 90, 71 (1975).

20. Reported by K. Hanson, Proc. of the Lepton-Photon Symposium (1975).

21. R. Anderson et al., Phys. Rev. Lett. 30, 627 (1973).

22. This is discussed in M. Davier's lectures, ref. 2.

23. See, e.g., T. Uematsu, RIFP preprint 228, Kyoto University (1975) for a detailed comparison with experiment. Uematsu shows that the assumptions of power law scaling, the Mandelstam representation and exoticity leads to the CIM forms for the angular distribution.

24. A. Hendry, Phys. Rev. D10, 2300 (1974).

25. B. Schrempp and F. Shrempp, Nucl. Phys. B60, 110 (1973), Phys. Letters 55B, 303 (1975).

26. F. Elvekjaer, CERN preprint TH 2067 (1975).

27. S. Brodsky, Proc. Free Body Conf., Quebec (1974), SLAC-PUB-1497.

28. R. Arnold et al., SLAC-PUB-1596 (1975), Phys. Rev. Lett. 35, 776 (1975).

29. B. Chertok, private communication.

30. R. Blankenbecler, S. J. Brodsky, and J. Gunion, SLAC-PUB-1585 (to be published in Phys. Rev.).

31. J. Cronin, Proc. Summer Inst. on Particle Physics, SLAC, 1974.

32. H. Fried, et al., Brown University preprint (1974), and references therein.

33. D. Scott, Nuovo Cimento 78A, 271 (1973), Nucl. Phys. B74, 524 (1974).

34. J.D. Bjorken and J. Kogut, Phys. Rev. D8, 1371 (1973).

35. E. D. Bloom and F. J. Gilman, Phys. Rev. Lett. 25, 1140 (1970).

36. S. D. Drell and T. M. Yan, Phys. Rev. Lett. 24, 181 (1970); G. B. West, Phys. Rev. Lett. 24, 1206 (1970).

37. S. J. Brodsky, Proc. of the Summer Inst. on Particle Physics (1974).

38. S. J. Brodsky, J. Gunion, and R. Jaffe, Phys. Rev. D6, 2487 (1972).

39. J. Kiskis, Phys. Rev. D10, 1219 (1974).

40. D. Caldwell et al., private communication.

41. S. Brodsky, C. Carlson, R. Suaya, in preparation.

42. R. Raitio, and G. Ringland, in preparation.

43. G. Ringland, Proc. of the Summer Inst. on Particle Physics (1975).

44. J. Gunion et al., in progress.

45. A. P. Contogouris and D. Schiff, CERN preprint 2029 (1975).

46. F. W. Anderson et al., Phys. Rev. Lett. 34, 294 (1975).

47. J. Alonso and A.C.D. Wright, to be published in Phys. Rev. D12 (1975).

48. R. Blankenbecler, S. J. Brodsky, R. Savit and J. Gunion, Phys. Rev. D8, 4117 (1973), Phys. Rev. D10, 2153 (1974).

49. L. J. Gutay et al., BNL preprint (1975).

50. J. Cornwall and G. Tiktopolus, UCLA preprint (1975).

51. P. V. Landshoff, Phys. Rev. D10, 1024 (1974).

52. J. C. Polkinghorne, Phys. Lett. 49B, 277 (1974).

53. T. Appelquist and F. Poggio, Phys. Rev. D10, 3280 (1974).

54. P. Menotti, Phys. Lett. 56B, 169 (1975), and preprint SNS 8/1975, and references therein.

55. A. M. Polyakov, Proc. of the Symposium on Lepton-Photon Iterations, SLAC (1975).

56. F. Salpeter, Phys. Rev. 87, 328 (1952).

57. See, e.g., reference 48. I wish to thank H. Harari for discussions on this point.

58. J. D. Bjorken (private communication).

59. This has been recently emphasized by T. Uematsu, ref. 23.

60. See S. Brodsky, F. Close and J. Gunion, Phys. Rev. D8, 3673 (1973), and references therein.

61. See, G. Farrar, Caltech preprint CALT 68-478 (1975), J. Pumplin and E. Yen, Michigan preprint (1975).

62. J. Kuhn, SLAC-PUB-1633, 1975.

63. N. N. Nicolaev and V. I. Zakharov, Phys. Letters 55B, 397 (1975).

64. S. Brodsky and J. Kuhn (in preparation).

65. I wish to thank J. Bjorken for discussions on this point.

66. S. Brodsky and D. R. Yennie (unpublished).